Do Sabellaria alveolata reefs act as nursery areas for juvenile fish? First evidence from the integration of drone-based imagery and underwater visual census data

Daniele Ventura[1*], Stanislas F. Dubois[2], Edoardo Cardella[1], Francesco Colloca[3], Francesco Tiralongo[4], Arnold Rakaj[5], Andre Bonifazi[5], Giovanna Jona Lasinio[6], Emanuele Mancini[7], Iacopo Bertocci[8], Edoardo Casoli[1], Gianluca Mancini[1], Tommaso Valente[1], Andrea Belluscio[1], Giandomenico Ardizzone[1], Maria Flavia Gravina[5]

[1*] Department of Environmental Biology, University of Rome 'La Sapienza', V. le dell'Università 32, 00185 Rome, Italy Daniele.ventura@uniroma1.it

[2] IFREMER, DYNECO-LEBCO, Centre de Bretagne, Technopole Brest-Iroise, 1625 route de Sainte-Anne, CS 10070, Plouzane 29280, France

[3] Department of Integrative Marine Ecology, Stazione Zoologica Anton Dohrn, Rome, Italy

[4] Department of Biological, Geological and Environmental Sciences, University of Catania, 95129 Catania, Italy

[5] Department of Biology, University of Rome 'Tor Vergata', Via della Ricerca Scientifica s.n.c., 00133, Rome, Italy

[6] Department of Statistical Sciences, University of Rome 'La Sapienza', V. le dell'Università 32, 00185 Rome, Italy

[7] Department of Biological and Environmental Sciences and Technologies, DiSTeBA, University of Salento, 73100 Lecce, Italy

[8] University of Pisa, CoNISMa, Via Derna 1, Pisa, Italy

Running page head: Nursery role of *Sabellaria alveolata* reef

Key words: fish habitats, habitat complexity, biogenic reef, UAVs, Mediterranean Sea

Abstract

The biogenic reefs built by the honeycomb worm *Sabellaria alveolata* constitute priority habitats along Atlanto-Mediterranean coastal areas. Despite their wide extent and important ecological role, the nursery value of *S. alveolata* reefs remains unclear, and more information is needed to define how such structured habitats affect juvenile fish assemblages. In this study, the habitat use of seven juvenile fish species was investigated by underwater visual census (UVC) in three study sites representing a gradient of complexity of *Sabellaria* reef habitats, spanning from a large and uniform

reef to patchy and isolated small reef formations. Sabellaria reef metrics derived by drone-based cartography and GIS analysis were used to quantitatively monitor the seasonal structural changes occurring due to the natural dynamics of the reefs. We also tested the potential effect of *Sabellaria* habitats on the growth and relative condition factor (K_n) of the *Diplodus sargus* juveniles. Five of the seven surveyed species, especially sparid fishes, showed a clear preferential association with *Sabellaria* formations. The generalized additive model (GAM) revealed a significant effect of the Compactness Ratio on estimated fish densities at high and low index values. The juveniles sampled on *Sabellaria* reefs exhibited higher values of K_n than those sampled on rocky habitats, supporting the hypothesis that structural complexity positively affected the condition. We provided evidence on habitat use by juveniles, suggesting that the presence of the *Sabellaria* reef may act as a nursery and affect local fish density in Mediterranean coastal waters.

1. INTRODUCTION

Marine coastal habitats provide several ecosystem services to nearshore human populations, including shoreline protection, commercial fisheries, recreational activities, and nutrient cycling. The ecosystem goods and services provided by coastal habitats, such as seagrass beds, estuarines mudflats, and saltmarshes are appreciably higher per unit area than those provided by terrestrial habitats (Costanza et al. 1997, Lefcheck et al. 2019). Coastal marine ecosystems encompass highly productive areas such as estuaries and bays that provide food resources and refuge for adult and juvenile fish and invertebrate species, contributing significantly to local and global biodiversity. As a result, they are widely recognized as nursery grounds for the growth and development of juvenile fish and shellfish (Paterson & Whitfield 2000, Beck et al. 2003). Over the last decades, a great effort was made to define a standard framework to rigorously measure the importance of juvenile habitats as nurseries and to support their protection (Beck et al. 2003, Dahlgren et al. 2006, Nagelkerken et al. 2015). The Nursery Role Hypothesis (NRH) formalized by Beck et al., (2001) states: ‘a habitat is a

nursery for juveniles of a particular species if its contribution per unit area to the production of individuals that recruit to adult populations is greater, on average, than production from other habitats in which juveniles occur'. This definition constitutes a standard framework for rigorously measuring, comparing, and categorizing nursery habitats through the ecological processes capable of supporting greater contributions to adult recruitment, depending on any combination of four factors: (i) density, (ii) growth, (iii) survival of juveniles and (iv) movement to adult habitats. Therefore, the concept of a nursery must extend beyond simply the numbers of juveniles present but also may entail higher specific growth rates due to the abundance of food resources, higher survival owing to protection from predators, and effective juvenile-adult linkage, resulting in more juveniles reaching the adult population (Heck Jr et al. 2003). Although some aspects of the NRH have been contested (Sheaves et al. 2006, Baker & Sheaves 2007) and some modifications, therefore, suggested (Dahlgren et al. 2006, Nagelkerken et al. 2015), the core framework provided by NRH for measuring juvenile habitat quality remains widely agreed upon. However, despite wide acceptance of NHR by marine biologists, fisheries managers and other stakeholders, and its recurrent use as justification for the protection and conservation of these specific widely distributed nursery habitats such as seagrass beds, estuaries, saltmarshes, mangroves forests, oyster beds, and shallow rocky reefs (Nagelkerken et al. 2002, Dahlgren et al. 2006, Nagelkerken 2009, Litvin et al. 2018), few attentions have been dedicated to other less common coastal habitats that can yet play an important role in ecosystem functioning at the local scale. Among these, the role played by temperate biogenic reefs made by the polychaetes of the genus *Sabellaria* (Annelida, Sabellariidae) for the juvenile fish remains unevidenced and poorly documented. The honeycomb worm *Sabellaria alveolata* (Linnaeus, 1767) is a common filter-feeding gregarious species that builds wave-resistant reefs of various types (i.e. mushrooms, pillows, barriers, and platforms; Curd et al. 2019) by assembling mobile sand grains into solid tubes (Le Cam et al. 2011, Lisco et al. 2017). These worms

84 collect with specific tentacular filaments calibrated sediments and bioclast particles between 63 µm
85 and 2 mm (belonging to the ‘sand‘ class on the Wentworth scale), resuspended by wave action, that
86 are then cemented with proteinaceous adhesives to create a rigid but elastic tube (Le Cam et al.
87 2011, Deias et al. 2023). Due to their ability to transform soft-sedimentary habitats into engineered
88 hard bioconstructions and to modulate resource availability to other species via structural
89 modifications of the environment, *Sabellaria* worms are defined as 'ecosystem engineers' (Jones et
90 al. 2018, 2021). *Sabellaria* reefs are widespread along European Atlantic coasts, occurring on
91 intertidal and subtidal shores of west Scotland to the south of Morocco (Dubois et al. 2002, Firth et
92 al. 2015, Curd et al. 2019). In the Mediterranean Sea, important sabellariid reef formations can be
93 found along the peninsular Italian coast (Gravina et al. 2018, Ingrosso et al. 2018, Bonifazi et al.
94 2019) and Sicily (Borghese et al. 2022, Sanfilippo et al. 2022), where they occur
95 from the lower shore to the sublittoral fringe. *S. alveolata* can be regarded as the most important
96 building organism along intertidal sandy coastal habitats, where it plays key ecological functions
97 such as creating biodiversity hotspots (Dubois et al. 2006, Jones et al. 2020, Muller et al. 2021),
98 increasing microphytobenthic primary production and promoting benthic-pelagic coupling (Jones et
99 al. 2021) or filtrating phytoplankton biomass resulting in high clearance rates (Dubois et al. 2003).
100 As a result, these reefs are listed under Annex I of the EC Habitats Directive (European Council
101 Directive 92/43 on the Conservation of Natural Habitats and of Wild Fauna and Flora) as a marine
102 habitat to be protected by the designation of 'Special Areas of Conservation'. Despite their relevant
103 ecological role, sabellarid reefs are listed as "Data Deficient" in the European Red List of Habitats by
104 the IUCN (Franzitta et al. 2022). While macrofauna biodiversity assemblages associated with
105 *Sabellaria* reefs are well investigated (Bonifazi et al. 2019, Muller et al. 2021), very little is known
106 regarding motile-associated megafauna using this habitat, especially fish assemblages. In this
107 context, defining the role of *S. alveolata* reefs in providing the specific ecosystem service of

supporting juvenile life stages and thus sustaining adult fish populations is a fundamental requirement for characterizing and better managing coastal areas. It is well known that habitat complexity provided by three-dimensional structures constructed by marine polychaete worms in the families Sabellariidae (*Sabellaria alveolata, S. spinulosa*) and Terebellidae (*Lanice conchilega*) can serve as nursery grounds for larvae of several invertebrate species (Dias & Paula 2001, Dubois et al. 2006, Bremec et al. 2013, Seitz et al. 2014, Bonifazi et al. 2019, Aviz et al. 2021). However, regarding fish species, only a few studies reported *L. conchilega* (Rabaut et al. 2010) and *S. spinulosa* (Pearce et al. 2011b a, Gibb et al. 2014) reefs as nursery grounds for certain fish species of commercial interest (i.e. flatfish) because the high abundance of juveniles hosted. Since the role of *S. alveolata* reefs as nursery grounds remains unclear, the main objective of this study is to assess if *S. alveolata* biogenic habitats play a key role in the Mediterranean fish population by investigating juvenile fish species' juvenile density, growth, and survival.

Over the past 50 years, a variety of *in situ* non-destructive underwater visual census (UVC) techniques have been used to quantitatively estimate relative abundances, densities, sizes, biomass, habitat types, and community structure of both adult and juvenile fish species in tropical (Brock 1954, Sale & Douglas 1981, Bohnsack & Bannerot 1986, St. John et al. 1990) and temperate areas (Harmelin-Vivien et al. 1985, 1995, Francour 1997, Vigliola & Harmelin-Vivien 2001, Cocheret De La Morinière et al. 2002, Ribeiro et al. 2005). Aside from the nature of the UVC method (e.g. point counts, strip transects, line transects, rapid visual counts) and the equipment used (e.g. SCUBA diving, baited remote underwater stereo-video stations, rotating video apparatus), UVC has proven helpful in expanding our knowledge in fish assemblages. However, no single approach is best suited for all circumstances, with each variant designed to examine a specific aspect of fish assemblages (Ribeiro et al. 2005). Moreover, the spatial distribution of juvenile fish assemblages is related to fine-scale variations in habitat structure (Harmelin-Vivien et al. 1995, Copp & Kovác 1996, Russo et

al. 2007, Ventura et al. 2015), making the presence of adequate habitats critical during the settlement of juvenile stages. As a result of this site-specificity determined by the availability of microhabitats, juvenile fishes typically show regular and predictable patterns of dispersal from the onset of settlement until recruitment to the adult population (Garcia-Rubies & Macpherson 1995). Therefore, it is crucial to integrate habitat surveys in UVC sampling to understand better organisms' distribution patterns in relation to available habitats. Using a combination of observational techniques, spatial monitoring surveys can provide a more comprehensive perspective on fish ecosystems, aimed at describing specific aspects linked to species and habitats association (Murphy & Jenkins 2010). Underwater imagery derived from single photographs and video sequences acquired by underwater cameras mounted on remotely operated vehicles (ROVs) and autonomous underwater vehicles (AUVs), as well as acoustic data (side scan sonar, multibeam echo sounders), represent the most employed remote observational techniques used to support UVC (Kenny et al. 2003, Chabot et al. 2017, Egerton et al. 2018, Wetz et al. 2020, Cheal et al. 2021). Emerging technologies and recent advances in aerial imagery, such as multispectral satellite imagery (Collin et al. 2017) and airborne light detection and ranging -LiDAR- (Collin et al. 2018b) have the potential to increase our ability to accurately map remote or inaccessible areas, improving habitat discrimination within complex reef seascapes at large spatial scales. Also, at a finer scale and more specifically regarding *Sabellaria* reefs, low-cost but promising unmanned aerial vehicles (UAVs) applications has been efficiently used to generate ultra-high spatial resolution orthophoto mosaic s of honeycomb worm reefs, using a photogrammetric approach (Collin et al. 2018a, 2019, Ventura et al. 2018a, Jackson-Bué et al. 2021). Although these cartographic outputs can guide fish censuses more effectively in identified habitats of interest and finely depict reef topography to reduce time and costs considerably in underwater surveys, no attempts have been made to connect such mapping efforts to direct UVC data. Considering that data on the recruitment of demersal coastal

156 fishes along the Italian coasts are still scarce and generally related only to the arrival of 0-group
157 fishes in bays or lagoons (Vigliola et al. 1998), without no quantitative information available for
158 specific microhabitat requirements such as those constituted by *Sabellaria* formations, we
159 examined patterns of habitat utilization by seven juvenile species. Therefore, we investigated for
160 the first time the role of *S. alveolata* reefs in providing an effective nursery habitat for juvenile fish
161 among coastal waters by integrating GIS information derived from drone-based cartography with
162 traditional UVC abundance estimates. We also explored the importance of *S. alveolata* reef
163 structure on the recruitment dynamics by associating the observed fish densities with reef shape
164 complexity measured during winter (bioconstructions in the retrograding phase) and summer
165 months (bioconstructions in the prograding phase). Finally, to provide a complete picture of the
166 NRH, we also investigated growth and body condition for the white seabream *Diplodus sargus*,
167 besides juveniles 'abundance patterns. The interest in this species was driven by its socioeconomic
168 importance being exploited in local/artisanal and recreational fisheries throughout the year (Biagi
169 et al. 2002, Tiralongo et al. 2021).

170

171 ## 2. MATERIAL AND METHODS

172

173 ### 2.1 Study site

174 This study was carried out along 1.3 km of sandy coastline in the Central Mediterranean Sea
175 (Tyrrhenian Sea, west coast of Central Italy) south of Anzio harbour, near the Natural Reserve of Tor
176 Caldara. Along this coast, water turbidity is high during most of the year because of fine sandy
177 sediments mixed with terrigenous particles derived from river runoff and high hydrodynamic force
178 (high exposure to winds and wave energy from the southern sectors), making the area suitable for

179 the settlement of *S. alveolata* which is well adapted to turbid systems and capable of maintaining
180 its filtering activity even under high seston loads (Dubois et al. 2003).
181 Three sampling sites (S1, S2 and S3, Fig. 1) were identified according to a gradient of structural
182 complexity of *S. alveolata* bioconstructions. Large ball-shaped structures (up to 2 m diameter), some
183 of them fused to form barriers and small platforms from the water surface up to 3 m depth,
184 characterized the reef at the S1 site (41°29'34.345 "N; 12°35'9.088 "E). Due to its persistence and
185 high ecological interest, this area has already been studied from geological (Moretti et al. 2019) and
186 biological perspectives (La Porta et al. 2009, Ventura et al. 2018a). A smaller *S. alveolata* reef, mainly
187 composed of mushroom-shaped formations (up to 1 m diameter) over a pebbly bottom from 0.5 to
188 3.5 m depth, characterized the S2 site (41°29'18.224 "N; 12°35'18.977 "E). The site S3 (41°29'13 "N;
189 12°35'19.172 "E) was characterized by reef type composed of isolated veneers and small pillow-
190 shaped hummocks over a calcareous (upper Plicocene bioclastic calcarenites) substrate. Sites S1 and
191 S2 mainly exhibited prograding formations (i.e. evidence of recent building activity and expanding
192 biogenic formations). In contrast, site S3 exhibited retrograding phases (i.e. evidence of degraded
193 reef portions and empty tubes), with biogenic formations showing signs of biofilm and epibiont
194 cover, also represented in the surrounding bedrock covered by a dense carpet of photophilous
195 algae. In this study, we cannot identify a standard control site with only rocky substrata since it is
196 not present along the coast, especially considering reasonable distances from the other two sites
197 (S1 and S2) where *Sabellaria* forms complex and stable reefs. In fact, the promontory at the S3 Site,
198 which presents only small and isolated portions of *Sabellaria* growing on rocks, is the only stretch
199 of coast with hard calcareous seabed. While areas displaying only rocky outcrops, such as Capo
200 Circeo and Capolinaro, are present at around 60 km southward and 80 km northward, respectively,
201 at such distances, other local factors related to oceanography and larval supply might have
202 influenced juvenile densities, masking the effects of habitat type.

2.2 UAV-based imagery and GIS analysis

In late September 2019, an aerial survey with a low-cost UAV (Quanum Nova CX-20 equipped with a GoPro Hero 8 action camera) was used to produce a coarse map of the coast from an altitude of 120 m to identify the three study sites (Fig. S1 in supplementary material). Subsequently, to effectively support the UVC survey, from October 2020 to November 2021, six high-resolution/low-altitude mapping missions were carried out both in fall-winter (September-February), following the main retrograding reef phase during autumnal storms and in spring-summer (March-August), following the main prograding reef phase after larval recruitment focused during the spring (Ventura et al. 2021). Mapping missions were carried out always with calm sea conditions and low wind < 1 knot (0-1 on the Beaufort scale) to ensure optimal detection of targeted habitats and low local turbidity. Aerial mapping was conducted from an altitude of 30 m using a modified DJI Mavic 2 Pro UAV equipped with an additional L1/ L2 GNSS receiver with Post Processing Kinematics (PPK) capabilities to provide an improved cartography in terms of spatial resolution and positional accuracies of the three sites. This consumer-grade off-the-shelf UAV was a lightweight (0.9 kg) and easy-to-carry (322 L × 242 W × 84 H mm) quadcopter equipped with a fully stabilized 3-axis gimbal Hasselblad L1D-20c camera RGB camera with a 1-inch CMOS sensor. Each Li-Po Battery (3850 mAh) offered up to 30 minutes of flight time with good weather conditions and low wind. Considering that the Mavic 2 Pro Hasselblad L1D- 20c camera produced 20 Megapixel format (5472 x 3648) photos, the sensor width was 13.2 mm, the actual focal length was 10.3 mm, and the UAV flew at a constant height of 30 m above the mean sea level (AMSL); we applied the following formula to estimate the ground sample distance (GSD, the distance between two consecutive pixel centres measured on the ground):

$$GSD_{cm/pix} = \left(\frac{Sensor\ width_{\ mm} \times Flight\ height_{\ m}}{Focal\ lenght_{\ mm} \times Image\ width_{\ pix}}\right) \times 100 \quad (1)$$

to get a GSD of 0.7 cm per pixel, allowing an excellent identification of above and below-water *S. alveolata* formations. The PPK routine was performed in Toposetter 2.0 Pro software, which allowed an accurate georeferencing (less than 10 cm-level accuracy in horizontal/vertical positioning) of the acquired imagery along the UAV track using as input the UBX files recorded by the L1/ L2 GNSS receiver mounted on the UAV and Rinex 3.03 files derived by a near Continuously Operating Reference Station (Ventura et al. 2023a).

The UAV-based imagery was processed using Agisoft Metashape v 1.6.1, a low-cost Structure from Motion (SfM) photogrammetric software, to generate orthorectified photomosaics of the study area. SfM outputs included Digital Surface Models (DSMs) of the mapped locations. Still, we did not include height information since the surface/elevation numerical model of the submerged part of the reef was affected by considerable inaccuracies due to water movements and light scattering. Orthophoto mosaics generated in Metashape were exported as raster images (GeoTIFF format, in the reference system WGS84/UTM zone 33 N, EPSG:32633) into a geographical information system using ArcMap 10.6 software (Esri 2011) for subsequent Object-Based Image Classification (OBIA). Before classification, we reduced the pixel complexity by segmenting the orthophoto mosaics into more compact image objects through the mean-shift (MS) segmentation function available in the Spatial Analyst extension (Ventura et al. 2022, 2023b a). The spectral details, spatial details, and minimum segment size parameters were set to 20, 18 and 800, respectively. After segmentation, we manually selected 30 image objects for each cover class (*Sabellaria* reef, sandy bottoms, and rocky substrata) as training samples to train the Support vector machine (SVM) algorithm. The SVM model uses each band's mean and standard deviation to classify the image objects in the whole dataset. The classification results were verified using confusion matrices to compare OBIA results against 50 assessment points (20 ground-truthed and 30 random points visually sampled on the orthophoto mosaic). Validation points were first compared with the resulting classification, and the

analyses included an overall map and per-class accuracies. We did not include the kappa coefficient because the chance agreement is irrelevant in an accuracy assessment (Foody 2020). After cover class identification through OBIA, the Patch Shape extension available in the opensource plugin WhiteBox Tools v.1.4.0 (Lindsay 2014) was used to add indicators of shape complexity to the identified *S. alveolata* polygons, using three complementary metrics: (1) the 'Compactness Ratio (CR)' which expresses the Area/Perimeter ratio, a measure of shape complexity, for vector polygon where an increase in fragmentation leads to an increase in perimeter more rapidly than a change in area and therefore a decrease in CR ; (2) the 'Shape Complexity Index (SCI)' which relates a polygon's shape to that of an encompassing convex hull, defined as SCI = 1 - A / Ah. Where A is the polygon's area, and Ah is the area of the convex hull containing the polygon. As the shape of the polygon becomes more complex, the SCI approaches 1, and (3) the 'Hole Proportion (HP)' which calculates the proportion of the total area of a polygon's holes relative to the area of the polygon's hull. It can be a valuable measure of shape complexity or a patch's discontinuity (Lindsay 2014). Mean values of CR, SCI and HP were derived using all the polygons attributed to *S. alveolata* reef for each study site and survey period. The percentage cover for each seabed class was calculated by dividing the area covered by the respective polygon by the total mapped area of the site. The aerial mapping mission was conducted using precise GPS information, ensuring that the total mapped area remained constant throughout summerly to winterly surveys.

2.3 Underwater Visual Census Sampling

Data on juvenile fish abundance and microhabitat use were collected twice per month from October 2020 to November 2021 by UVC. Censuses were carried out between 11:00 am and 3:00 pm and in the depth range of 0.3 - 2.5 m. To standardize the sampling effort, the UVC was carried out along

predefined pathways, previously defined on UAV cartography, with different lengths according to the extent and complexity of each site, to cover an area of 600 m^2 (200 m in length x 3 m in width) in sites S1 and S3 and an area of 570 m^2 (190 m L x 3 m W) in site S2. One snorkeler swam slowly following the reef border while simultaneously recording all individuals within a fixed distance of 1.5 m per side. This distance was chosen because of the limited maximum horizontal underwater visibility and the small sizes of juveniles. To follow the correct path during each UVC survey, the snorkeler was equipped with a real-time track system through a water-resistant tablet running the GPS LoggerPro App, directly mounted on the marker buoy. The number of individuals of seven target species (*Diplodus sargus, D. puntazzo, D. vulgaris, Salpa salpa, Dicentrarchus labrax, Umbrina cirrosa* and *Atherina hepsetus*), time of the day, tide level, and preferred habitat type according to two main categories (*S. alveolata* reef and hard substrata encompassing rocks with photophilic algae, pebbles, and gravel) were recorded. When juveniles were observed for more than 5 min on a specific substrate type, we considered it a preferred substratum, as young juveniles typically show a strong site-specificity, the microhabitat they were found in was assumed to be the one they preferentially used (Garcia-Rubies & Macpherson 1995, Macpherson 1998).

Size classes for sparid fishes were chosen to define three principal periods of juvenile ontogenetic development (Macpherson 1998, Vigliola et al. 1998): settlement phase (smallest juveniles, from 10 to 20 mm total length, TL), intermediate phase (medium-size juveniles, from 20 to 45 mm TL) and pre-dispersal phase outside the surveyed nursery areas (large-size juveniles, from 45 to 66 mm TL). For other species, fish sizes were recorded in 30 mm size intervals. Plastic tablets with fish silhouettes and a ruler attached to the end of a meter stick were used to reduce magnification errors in estimating fish length (Bohnsack & Bannerot 1986, Harmelin-Vivien et al. 1995). When large shoals were observed, the count was carried out later in the lab, using FULL-HD (1920 X 1080p)

298 frames captured from video footage acquired by a Sony Alpha 6000 camera within a Sea Frog
299 polycarbonate housing.
300
301 **2.3 Estimation of condition factor and growth of *Diplodus sargus***
302 To determine the role of S. *alveolata* reef on *D. sargus* juveniles' condition, 153 fish (ranging in size
303 from 16 to 66 mm TL) were collected monthly from May to August 2021 in the three sites, using
304 specific hand-nets with a 5 mm mesh size. We adapted the sampling effort proportionally to the
305 extent of the total cover of the habitats (i.e. *S. alveolata* reef dominant in sites S1 and S2 and other
306 hard substrates encompasses rocks, pebbles and gravel mainly represented in Site S3) to ensure
307 comparable fish samples between sites. Therefore, we collected *D. sargus* juveniles on *S. alveolata*
308 in S1 and S2 sites, whilst juveniles associated with rocky areas were sampled only from site S3.
309 Monthly size distributions of *D. sargus* juveniles were estimated for each sampling site and
310 preferential habitat to estimate growth variation over time. Considering the different extents of
311 each site's two main habitat types and the selective sampling method, the site could be used as a
312 proxy for associating juveniles with the two main habitat types (*Sabellaria* and rocky substrata).
313 Moreover, juveniles of *D. sargus* were never found free-swimming on sandy areas but always
314 sampled in small shoals, stationary in proximity to the two substrata considered. Covariance analysis
315 (ANCOVA) and linear regressions were used to test for slope differences between juvenile growth
316 rate and habitat type.
317 The relative condition factor K_n was used to study the variation in juvenile conditions while avoiding
318 the effect of length (Ferraton et al. 2007). For each specimen, the total length TL, in cm) and the
319 eviscerated wet body weight (We, in g) were used to compute the formula as follows:
320 $$K_n = \frac{We}{We'} \quad (2)$$

where *We* is the measured individual eviscerated weight and *We'* is the estimated eviscerated weight from the $\log_{10}We$ - $\log_{10}$TL relationship ($We' = 10^{-intercept} \times TL^{slope}$).

2.4 Data Analysis

Juvenile fish densities (D, expressed in the number of juveniles per 100 m^2) were estimated using UVC data as follows:

$$D_i = \frac{n_i}{W*L} \quad (3)$$

where n_i is the number of individuals detected, W is the path width (in metres), and L is the path length (in metres). Generalized additive models (GAMs) were used to investigate the influence of reef metrics on juvenile fish densities among the three study sites. GAMs are non-parametric extensions of generalized linear models (GLM) that allow for non-linear relationships between predictor and response variables common to ecological data (Guisan & Zimmermann 2000, Zuur et al. 2007). The following equation gives general GAM construction:

$$\mathrm{E}[\mathrm{Y}|\,\mathbf{X}] = \mathrm{g}^{-1}(\mathbf{X}_\mathrm{a}\boldsymbol{\beta} + \textstyle\sum_\mathrm{k} \mathrm{s}\,(\mathrm{X}_\mathrm{k})) \quad (4)$$

where E[Y|**X**] is the expected value of the response variable (log-transformed fish densities) given all independent information, g is a link function, $\mathbf{X}_a$ is a set of predictors linearly related to the dependent variable. At the same time, X_k represents one of the K predictors not linearly related to the dependent variable, and S_k is a smooth function of the predictor variable, X_k. A GAM with Gaussian distribution (with identity link function) was fit with a cubic regression spline as a smooth function using the 'mgcv' library in R version 4.2.1 (Wood 2001). Smooth functions were used to model the relationship between the response variable and the reef metrics estimated from UAV-based cartography. In the current study, cubic splines were restricted to a maximum of 5 knots for the full set of independent variables (i.e. site, species, size class, season, tide level, *Sabellaria* reef cover, substratum type, CR, SCI, and HP) to prevent overfitting (Dance & Rooker 2016). Independent

345 variables influencing juvenile densities were selected for the final model using a backwards stepwise
346 procedure based on minimizing the Akaike information criterion (AIC), which measures goodness of
347 fit while accounting for model complexity (number of variables). The approximate significance of
348 the smoothed predictor (p-values) was used to guide the backward selection procedure, where the
349 variable with the highest p-value (above 0.05) was removed first. When removing a predictor
350 returned model with a smaller AIC (with ΔAIC > 2 between models), the same variable was excluded
351 from the analysis. Stepwise selection continued until removing any remaining predictors increased
352 in the model AIC (Anderson et al. 1998). Non-significant ($p > 0.05$) terms retained in the final model
353 were removed if model AIC was comparable (<2) after removal. In addition, as a secondary criterion
354 to AIC, the overall model fit was assessed with percent deviance explained: DE = [(null deviance −
355 residual deviance) / null deviance] × 100. The relative influence of each independent variable was
356 assessed by removing each variable individually from the final model and comparing the percent
357 change in DE (ΔDE) and change in AIC (ΔAIC). The 'gam.check' tool of the 'mgcv' package (Wood &
358 Wood 2015), which plots the deviance residuals against approximate theoretical quartiles of the
359 residual deviance distribution according to the fitted model, was used to check the model's
360 residuals. Models with overdispersed and anomalous distribution of residuals were discarded.
361 Significant differences for either fish habitat/site association and K_n were tested with the non-
362 parametric Wilcoxon signed rank test using the ‘wilcox.test’ function in the ‘rstatix’ package. The
363 Bonferroni correction was applied to the resulting p-values to account for the influence of multiple
364 tests. Results of the tests, expressed with significance codes, were reported directly on plots using
365 'ggpubr' and 'ggsignif' R packages (Kassambara 2020, Ahlmann-Eltze & Patil 2021).
366

367 **3 RESULTS**

368 **3.1 *Sabellaria* reef metrics and their relationship with juvenile densities**

The UAV-based orthophoto mosaics generated after SfM processing showed a spatial resolution of 0.66 cm/pix (Fig. 2 a-d and Fig. S2 supplementary material). The high level of detail supported the UVC sampling by providing the snorkeler with accurate cartographic support that was helpful for survey management and data acquisition. The OBIA classification approach effectively identified the most important features of the coastal zones, including *Sabellaria* reefs, resulting in an overall mean (± SD) accuracy of 86.9 % (± 0.3). Major land-cover misclassification errors involved spectral confusion among the class 'rocks with algae' with a total of 8.16% and 16.3% of samples interpreted as *S. alveolata* reef and sandy bottoms, respectively (Overall, producer and user accuracies are reported in Table S1 of the supplementary material). *S. alveolata* reef cover in S1 (Wilcoxon signed-ranks test; W = 3986, p-value = 0.0001) and S2 (Wilcoxon signed-ranks test; W = 2257, p-value = 0.01) sites significantly differed from S3 site considering both the winter and summer months. The S1 site exhibited the most considerable reef extent (2056 m^2) in summer, covering more than 33% of the whole area, whilst only limited *S. alveolata* reef bioconstructions were reported in the S3 site, with an average cover of 5.2% throughout the year (Table 1). Generally, we observed a reduction in *S. alveolata* reef cover (up to 10% in the S1 site) with an increase in the areas covered by sandy bottoms from summer to winter due to natural erosion of the bioconstructions and sand deposition during severe storms occurring more frequently from late summer.

S. alveolata reef metrics Compactness Ratio (CR)', 'Shape Complexity Index (SCI)' and 'Hole Proportion (HP)', derived after polygon delineation based on OBIA classification, exhibited large habitat variability among sites and seasons (Fig. 3). Generally, the three metrics reported significative differences from summer to winter months, denoting their ability in detecting natural dynamics of *S. alveolata* reefs. The S1 site showed the highest CR among the studied reefs both in summer and winter, being well-structured with a compact shape denoting reef stability. High CR values in the S1 site corresponded to a reef composed of large and continuous colonies (high surface

for low perimeter) that can offer a more stable structure capable of withstanding the intensity of wave action and little prone to retrograding phase in winter. As expected, smaller CR values indicated smaller and more fragmented reef structures at sites S2 and S3. Consequently, SCI increased significantly in S1 (Wilcoxon signed-ranks test; W = 266, p-value < 0.001) and S2 (Wilcoxon signed-ranks test; W = 589, p-value < 0.001) sites from summer to winter, highlighting reef fragmentation. Conversely, site S3 showed larger values of SCI in winter because of isolated reef formations constituted by small and low veneers between rocks, offering limited surfaces exposed to waves and therefore less prone to damage (Curtis 1975). In the S1 and S3 sites, HP did not significantly increase in winter, whilst hole formation significantly (Wilcoxon signed-ranks test; W = 560, p-value < 0.001) occurred in *S. alveolata* reefs in the S2 site.

The final selected GAM model (DE = 64.9% and pseudo-R^2 = 0.62) fitted on 256 observations included four retained variables, with species, site, size class, and CR resulting as the most influential (Table 2). This model includes information on all relevant sources of variability when referring to the juveniles' density. The GAM formula we chose according to the AIC selection procedure and diagnostic plots were reported in the supplementary material as Equation S1 and Figure S3, respectively.

For all the considered species, densities showed a significant negative effect from site S1 to S3, which is especially marked for sparid species (higher for *Diplodus* spp. and minimum for *Salpa salpa*), *D. labrax* and *U. cirrosa*. Among *Diplodus* species, the white seabream *D. sargus* seemed the most influenced in terms of site selection, similar to *D. labrax*. The response plot of the non-linear term showed a sinusoidal trend indicating that juvenile fish densities were lowest at moderate values (0.3-0.5) of *Sabellaria* reef CR, whilst larger densities were reported both at lower (< 0.3) and higher (> 0.5) CR values (Fig. 4).

3.2 Temporal and spatial variability of juvenile fish

A total of 3395 juveniles belonging to the seven target species were censused among the three sites over the whole study period. The most abundant species were two sparid fishes (*Diplodus vulgaris* and *D. sargus*), accounting for 32.3 % and 27 % of the total juvenile assemblage, followed by Atherinidae (*Atherina hepsetus*, 21.2%) and *Salpa salpa* (10.5%). *Diplodus puntazzo*, *Umbrina cirrosa* and *Dicentrarchus labrax* were reported occasionally, representing a small fraction of the assemblage (5.8%, 2% and 1.3%, respectively). Within-month variation of juveniles' density was high, especially for sparid fishes (Fig. S4 Supp. material). *Diplodus sargus* and *D. vulgaris* were found mainly from late spring to mid-summer, whilst *S. salpa* and *D. puntazzo* were observed in winter. The other species (*A. hepsetus*, *D. labrax* and *U. cirrosa*) were censused mainly in late summer or early autumn.

During summer months, juvenile density significantly differed from S1 to S2 sites (Wilcoxon signed-ranks test; W = 3399, p-value < 0.001) and from S1 and S3 sites (Wilcoxon signed-ranks test; W = 3554, p-value = 0.003), with the highest average (± SD) density of 14.3 ± 16.8 (n = 82) Ind. 100 m^{-2} recorded in the S1 site (Fig. 5). The sea breams *D. sargus* (Wilcoxon signed-ranks test; W = 1645, p-value < 0.001) *D. puntazzo* (Wilcoxon signed-ranks test; W = 129, p-value = 0.01) and the sea bass *D. labrax* (Wilcoxon signed-ranks test; W = 27, p-value = 0.04) showed significant decreasing density values passing from S1 to S3 sites (Fig. 6). The shi drum (*U. cirrosa*) juveniles were reported only in the S1 site. The other sparid fishes (*D. vulgaris*, *S. salpa*) and the Mediterranean sand smelt (*A. hepsetus*) were censused with comparable mean densities in all sites.

3.3 Juveniles' habitat use

The three juvenile species of the genus *Diplodus* (*D. sargus, D.vulgaris, D. puntazzo*)showed a significant association with *S. alveolata* biogenic formations when compared to the other rocky

habitats, mainly constituted by hard substrates covered by photophilic algae (Fig. 7). *U. cirrosa* juveniles were only reported in proximity to *S. alveolata* formations. Conversely, the mean densities of *A. hepsetus*, *D. labrax*, and S*. salpa* juveniles did not differ among the two habitat types, with the latter mostly forming large shoals over rocky substrates. Small and medium-sized juveniles (2-5 cm TL) were observed prevalently (> 70%) near *Sabellaria* formations (Fig. 8). This habitat association was particularly evident for sparid species (especially for *D. sargus*) and *D. labrax* being almost all the juveniles observed on *Sabellaria* reef, also several months after settlement. By contrast, large-sized juveniles of *S. salpa* (7-8 cm TL) and *A. hepset*us (2-3 cm TL) showed a preference for rocky substrates covered by photophilic algae.

3.4 Relative condition factor (K_n) and growth of *Diplodus sargus* juveniles

Monthly size distributions of the sampled *D. sargus* juveniles from May to August differ significantly between months and substrate type (Fig. 9 a) in June (Wilcoxon signed-ranks test; W = 286, p-value < 0.001) and July (Wilcoxon signed-ranks test; W = 55, p-value = 0.004). *D. sargus* juveniles associated with *Sabellaria* reef in S1 and S2 sites exhibited higher increases in monthly size (regressions' slopes were significantly different among habitat types in both slopes and intercepts (ANCOVA, regression slope: F = 4.33, df = 1, p = 0.03) than juveniles settling on other hard substrates in the S3 site (Fig. 9b).

The K_n significantly differed (Wilcoxon signed-ranks test; W = 1396, p-value < 0.001) in juvenile *D. sargus* living near *Sabellaria* reef compared to specimens collected on hard rocky substrates. These differences were particularly strong among small-sized (25.3 ± 3.1mm TL; Wilcoxon signed-ranks test; W = 70, p-value < 0.001) and medium-sized (35.1 ± 4.8 mm TL; Wilcoxon signed-ranks test; W = 63, p-value = 0.01) juveniles, whilst for larger juveniles (55.1 ± 4.7 mm TL), the effect of habitat on fish condition was not significant (Fig. 10).

3 DISCUSSION

The function of shallow coastal habitats as essential nursery grounds for marine fishes has become an accepted ecological concept (Amara et al. 2007, Searcy et al. 2007). However, not all coastal areas are equally important as nursery grounds. Quality nursery habitats contribute disproportionately to the adult population by supporting increased densities, faster growth, better survival, and successful movement of recruits to adult habitats (Beck et al. 2001). Juvenile fish densities, growth, survival, and connectivity are essential indicators of juvenile habitat quality that must be understood in an ecosystem-based approach to implementing comprehensive fisheries management strategies (Beck et al. 2003, Schloesser & Fabrizio 2019). Therefore, the dynamics affecting essential fish habitats must be recorded accurately and extensively in marine monitoring surveys, especially in complex coastal environments where microscale variability may affect the estimates (Edgar et al. 2004). To date, this assessment is generally missing for temperate biogenic reefs made by the tube-building worm *S. alveolata*, which, analogously to other biogenic worm reefs, are considered hotspots of biodiversity capable of providing refuge to an array of organisms, including hard and sandy bottom invertebrates (Bremec et al. 2013, Gravina et al. 2018, Ingrosso et al. 2018, Giangrande et al. 2020).

Our results indicated that juveniles of five commercially important species (*Diplodus* sargus, *D. puntazzo* and *D. vulgaris*, D. *labrax* and *U. cirrosa*) made a preferential use of *S. alveolata* reef habitats with more cohesive reef structures with little or no fragmentation as those occurring in the S1 site. Fish densities were non-linearly linked to the compactness ratio (CR) metric, a common estimate of the reef fragmentation: higher densities of juveniles were associated with high and low levels of reef CR, with lowest densities at moderate CR values. As expected, a massive, unfragmented, and compact reef (i.e. high CR values) has the greatest effect on the density and diversity of juvenile fish. It offers shallow, sheltered areas with reduced hydrodynamic forces and

lower predation rates (Ruiz et al. 1993). Paradoxically, a similar refuge effect can also be observed when reef habitat fragmentation is maximal (i.e. low CR values) due to an increase of faults and anfractuosities due to biogenic structures degradation (Dubois et al. 2002, Stone et al. 2019). This effect has been demonstrated in macrofaunal diversity, where numerous small sessile epibionts colonized degraded and fragmented reef structures (Dubois et al. 2006, Bonifazi et al. 2019). Similarly, as shown in degraded coral reefs, prey vulnerability increases, leading to an initial rise in resource availability and productivity for a significant part of the reef fish community, particularly herbivores and invertivores (Brandl et al. 2016, Olán-González et al. 2023), confirming that habitat degradation allows the exploitation of novel resources by fishes that feed on macroinvertebrates such as juvenile sparid fishes (Ventura et al. 2017, 2018b).

Moreover, when the loss of one microhabitat type occurs due to reef degradation during winter storms, there is a simultaneous replacement by another microhabitat type, and, typically, massive *S. alveolata structures* are replaced mainly by sandy rubble on degraded reefs, and some juvenile fishes that prefer rubble microhabitats benefit from reef degradation. On the other hand, the lowest densities of juveniles reported at moderate CR values may be due to the transitional morphology of the reef between prograding and retrograding stages (Curd et al. 2019, Firth et al. 2021). This study shows that the refuge effects of *S. alveolata* habitats are just as important whether the reef is massive and little fragmented or made up of small, highly fragmented structures, providing valuable nursery grounds hosting high juvenile densities throughout the year. This result should have consequences in terms of management and restoration (Franzitta et al. 2022) of this reef habitat so as not to target exclusively extensive reefs (in size or surface area). Still, it should also make it possible to justify important ecological functions in nursery areas for the smallest and most fragmented biogenic reefs.

512 It should be noted that the predicted effect size is minimal (approximately 5 fish per 100 m^2),
513 especially considering the considerable measurement uncertainty characterizing UVC sampling.
514 Moreover, the limited deviance explained by the CR term also suggested that the relationship was
515 not particularly strong. While accepting that structure does not significantly affect juvenile fish
516 densities at the scales and extents examined here, our results confirmed that the reef, in all its
517 forms, acts as a preferential habitat for juveniles. Consequently, we can argue that *S. alveolata* reefs
518 play an essential role as a nursery area for juvenile fish even though its degree of compactness and
519 fragmentation. Similar results are reported for plant traits such as shoot density and aboveground
520 biomass, which are only weakly correlated with the diversity of the associated fauna and may not
521 provide good proxies for diversity for another engineered habitat constituted by eelgrass (*Zostera*
522 *marina*) meadows (Muller et al. 2023). In fact, no significant differences were found between
523 communities from the centre to the edges of the meadows, indicating that both habitats provide
524 similar benefits to biodiversity and highlighting that the shape of the community was directly
525 mediated by the presence of the meadow more than its health status (Muller et al. 2023).
526 Estimates of the ecological values of nursery areas, which are particularly important in monitoring
527 the effects of fishing and protection strategies on the structure of coastal fish assemblages, are
528 available for a variety of coastal benthic systems, including those supported by engineering species
529 such as seagrasses (Jackson et al. 2001, Dorenbosch et al. 2004), mangroves (Mumby et al. 2004),
530 oyster reefs (Beck et al. 2003) and other reef-building polychaetes such as *Lanice conchilega* (Rabaut
531 et al. 2009, 2010), *Ficopomatus enigmaticus* (Méndez Casariego et al. 2004) and *S. spinulosa* (Reise
532 2012, Tillin & Gibb 2018). By contrast, virtually no data are available to quantify the importance of
533 *S. alveolata* formations for coastal juvenile fish assemblages, especially in the Mediterranean Sea.
534 Therefore, considering that the most common and widely accepted criterion for defining the nursery
535 function of habitats is their ability to provide food and refuge (Paterson & Whitfield 2000), the

efforts directed at evaluating habitat quality in the context of the nursery-role concept should not be limited to abundances, but should also take into account growth, survival and linkage (Beck et al. 2001, 2003, Dahlgren et al. 2006, Lefcheck et al. 2019). In this respect, we also evaluated the potential effects on growth rate and fish condition exerted by *S. alveolata* reefs compared to adjacent hard substrata. Fish condition is critical because it dramatically influences growth, reproduction and survival. Fish condition has seldom been used to assess habitat quality in marine ecosystems, where most of the research dealt with differences in abundance and biomass between habitats (Lloret et al. 2002, Cantafaro et al. 2017). Although we quantified growth and K_n for a single sparid species (i.e. *D. sargus*), our results provided an important baseline for other species that utilized the *S. alveolata* reef as a nursery area. *S. alveolata* reef hosts a high diversity of associated fauna, including sessile (bivalves), burrower (tanaidaceans) and infaunal (isopods, amphipods and polychetes) invertebrates, which could themselves support other benthic infaunal assemblages and, in turn, provide food for fish, as confirmed by previous studies on feeding habits of sparid fishes (Sala & Ballesteros 1997, Costa & Cataudella 2007, Ventura et al. 2017, Bonifazi et al. 2018). The highest K_n and growth rate were reported for small and medium-sized classes of juveniles, as larger juveniles already expand their feeding ground outside the reef structures: the high density in small invertebrates offers a head start in development for fish juveniles exploiting reef habitat as a feeding ground. The species *S. alveolata* is also a potential food source that may direct influence the condition of fish: worms can be sucked out from their tube by juveniles with enough suction power, such as sparids (Christensen 1978) or during reef destruction (i.e. during storms and periods of high wave energy). Considering, however, that juveniles of predators (*D. labrax*) were found in the same sites, the refuge effect from consumer pressure provided by shallow bottoms may be overestimated, suggesting that the refuge paradigm may be too simplistic for diverse and complex nursery grounds (Baker & Sheaves 2007). Thus, the factors that more likely influence the distribution

560 of juvenile fishes in shallow water are probably related to the availability of food resources (Le Pape
561 & Bonhommeau 2015).
562 In Mediterranean environments, especially inside complex communities such as seagrass meadows
563 and biogenic reefs, UVC results can be affected by some typical sources of error linked to
564 environmental conditions, such as water clarity that may affect the detectability of fishes (La Manna
565 et al. 2021), the surveyed area dimensions (Jones et al. 2015), the census methodology (Pais &
566 Cabral 2018), the trait of target fishes with different behaviour (Kulbicki 1998, Pais & Cabral 2017),
567 intra-observer variability due to divers' experience, and habitat spatio-temporal variability and
568 complexity (Friedlander & Parrish 1998, De Girolamo & Mazzoldi 2001, Green et al. 2013, Kislik et
569 al. 2020). This latter aspect deserves particular attention in planning accurate UVC monitoring to
570 estimate the specific association between juvenile fish and microhabitats, likely occurring at small
571 spatial scales (Harmelin-Vivien et al. 1995, Ventura et al. 2015, 2018b). In this context, recent
572 mapping technologies based on ultra-high resolution imagery acquired by small UAVs coupled with
573 OBIA classification can be a valuable tool in identifying and characterizing coastal areas (Goncalves
574 & Henriques 2015, Papakonstantinou et al. 2016, Ventura et al. 2016, 2018a, 2023b, Jeong et al.
575 2018, Adade et al. 2021), providing accurate GIS data of heterogeneous stretches of coasts where
576 the environmental variability of the seabed is a critical aspect capable of influencing the distribution
577 of juvenile and adult fish assemblages. We demonstrated that the use of UAV-based cartography
578 could be a valuable tool to integrate UVC surveys considering both the spatial planning of sampling
579 campaigns and data acquisition of geomorphological features related to specific habitats such as
580 sabellariid reefs that are characterized by high spatial 2D/3D heterogeneity, even at small spatial
581 scales (Bertocci et al. 2017, Jackson-Bué et al. 2021, Ventura et al. 2021). The potential of UAVs for
582 environmental assessment is increasingly being demonstrated, especially in monitoring
583 programmes of shallow marine habitats, which are more and more frequently carried out using

584 aerial UAV photography in conjunction with field surveys to map seagrass beds directly (Ventura et
585 al. 2018a), submerged aquatic vegetation (SAV) such as macroalgal beds (Rossiter et al. 2020,
586 Ventura et al. 2023b), coral reef (Casella et al. 2017, Collin et al. 2018b, Nguyen et al. 2021), rocky
587 reef (Tait et al. 2021) and other biogenic reefs (Collin et al. 2019, Donnarumma et al. 2021, Brunier
588 et al. 2022). Mapping and monitoring these habitats may provide valuable information on fish-
589 habitat associations, eventually helping to identify optimal monitoring designs and to establish the
590 most effective schemes of temporal and spatial acquisition of data to achieve the specific objectives
591 of the study, including, for example, the estimation of seasonal variability at target sites (Murphy &
592 Jenkins 2010). Although topographic features (e.g. Topographic Position Index, surface roughness,
593 slope) derived from elevation data (DEMs) were not explicitly considered here, they could provide
594 additional variables such as complementary fragmentation metrics or reef morphotypes descriptors
595 (Brunier et al. 2022) usable for the estimation of reef health status (Desroy et al. 2011, Bajjouk et
596 al. 2020). However, our approach demonstrated that RGB orthophoto mosaic and polygon
597 delineation in GIS could provide simple and relevant indicators of the shape and complexity of
598 *Sabellaria* reefs related to their potential role as nursery grounds for juvenile fish.
599
600 **4 Conclusions**
601 Using UAV-based cartography reveals the potential for high-resolution remote sensing imagery to
602 be implemented into traditional UVC-based monitoring efforts by quantifying biogenic reefs' fine-
603 scale attributes (Murfitt et al. 2017). The present study adds new perspectives to on-ground surveys,
604 giving insight into the distribution and abundance of juvenile species associated with complex
605 coastal habitats formed by reef-building polychaetes. The ability of UAVs to capture fine-scale (cm)
606 georeferenced imagery of the whole reef, depicting morphological changes occurring between
607 accretion and erosion processes due to environmental dynamics, is crucial for improving spatial

608 monitoring and assessing the spatial variability of reef habitat types. Although UAVs may not be able
609 to fully replace *in situ* monitoring techniques on sabellariid reefs, they can provide complementary
610 data suited to obtain a more comprehensive understanding of biogenic reef ecology and, in
611 particular, their nursery role. Because the nursery role concept aims to identify high-quality areas,
612 we encourage precise monitoring even on relatively small habitats, such as *Sabellaria* reefs
613 presented here. Despite their limited size, they can represent essential nursery habitats that can
614 support more adult recruits per unit of space compared to other habitats used by juveniles of the
615 same species. This is a crucial aspect for prioritizing spatially explicit management (e.g.
616 establishment of marine protected areas) when costs or other logistic constraints limit the amount
617 of space that can be protected (Dahlgren et al. 2006). Finally, although this study is relatively limited
618 in spatial coverage and temporal resolution and further studies are required to fully understand
619 connectivity and ecological habitat linkages (Nagelkerken et al. 2015), our findings can serve as a
620 starting point for examining the effects of *S. alveolata* bioconstructions on juvenile fish assemblages,
621 confirming that habitat structure should be included as a biodiversity component during evaluations
622 of its nursery role, especially under the predicted increase of the impact of human activities and
623 climate change on biogenic formations in the next few years (Dubois et al. 2006, Curd et al. 2023).
624
625 **Acknowledgements**
626
627 We are grateful to the ICES WGVHES working group for helpful discussion and advice on coastal
628 nurseries, especially Olivier Le Pape, Benjamin Ciotti, Elliot John Brown and David Eggleston. Thanks
629 to our friends and colleagues who provided support during fish sampling. We are indebted to
630 anonymous reviewers for valuable comments and suggestions. The small research grant (ID:
631 RP12117A53202425, entitled: 'Using unmanned aerial vehicles (UAVs) for 3D high-resolution
632 mapping of honeycomb worms *Sabellaria alveolata* (Annelida: Sabellariidae) reefs and assessment

of the associated fish assemblages' from Department of Environmental Biology and Ecology (University of Rome, 'La Sapienza') partially supported this research.

Bibliography

Adade R, Aibinu AM, Ekumah B, Asaana J (2021) Unmanned Aerial Vehicle (UAV) applications in coastal zone management—A review. Environ Monit Assess 193:1–12.

Ahlmann-Eltze C, Patil I (2021) Ggsignif: R Package for Displaying Significance Brackets for'ggplot2'.

Amara R, Méziane T, Gilliers C, Hermel G, Laffargue P (2007) Growth and condition indices in juvenile sole Solea solea measured to assess the quality of essential fish habitat. Mar Ecol Prog Ser 351:201–208.

Anderson DR, Burnham KP, White GC (1998) Comparison of Akaike information criterion and consistent Akaike information criterion for model selection and statistical inference from capture-recapture studies. J Appl Stat 25:263–282.

Aviz D, Santos CRM dos, Rosa Filho JS (2021) Sabellariid (Polychaeta: Annelida) reefs as nursery ground for the hermit crab Clibanarius symmetricus (Randall, 1840) on the Amazonian coast of Brazil. Mar Biol Res 17:21–30.

Bajjouk T, Jauzein C, Drumetz L, Dalla Mura M, Duval A, Dubois SF (2020) Hyperspectral and lidar: complementary tools to identify benthic features and assess the ecological status of Sabellaria alveolata reefs. Front Mar Sci 7:575218.

Baker R, Sheaves M (2007) Shallow-water refuge paradigm: conflicting evidence from tethering experiments in a tropical estuary. Mar Ecol Prog Ser 349:13–22.

Beck MW, Heck KL, Able KW, Childers DL, Eggleston DB, Gillanders BM, Halpern B, Hays CG, Hoshino K, Minello TJ (2001) The identification, conservation, and management of estuarine and marine nurseries for fish and invertebrates: a better understanding of the habitats that serve as nurseries for marine species and the factors that create site-specific variability in nurse. Bioscience 51:633–641.

Beck MW, Heck KL, Able KW, Childers DL, Eggleston DB, Gillanders BM, Halpern BS, Hays CG, Hoshino K, Minello TJ (2003) The role of nearshore ecosystems as fish and shellfish nurseries. Issues Ecol.

Bertocci I, Badalamenti F, Brutto S Lo, Mikac B, Pipitone C, Schimmenti E, Fernández TV, Musco L (2017) Reducing the data-deficiency of threatened European habitats: Spatial variation of sabellariid worm reefs and associated fauna in the Sicily Channel, Mediterranean Sea. Mar Environ Res 130:325–337.

Biagi F, Sartor P, Ardizzone GD, Belcari P, Belluscio A, Serena F (2002) Analysis of demersal fish assemblages of the Tuscany and Latium coasts (north-western Mediterranean). Sci Mar 66:233–242.

Bohnsack JA, Bannerot SP (1986) A stationary visual census technique for quantitatively assessing community structure of coral reef fishes.

Bonifazi A, Lezzi M, Ventura D, Lisco S, Cardone F, Gravina MFMF, Bonifazi A, Lezzi M, Ventura D,

669 Lisco S, Cardone F, Gravina MFMF (2019) Macrofaunal biodiversity associated with different
670 developmental phases of a threatened Mediterranean Sabellaria alveolata (Linnaeus, 1767) reef. Mar
671 Environ Res 145:97–111.

672 Bonifazi A, Ventura D, Mancini E (2018) Sabellaria reefs as reservoirs of preferential species: The case of
673 Eulalia ornata Saint-Joseph, 1888 (Annelida: Phyllodocidae). Mar Freshw Res 69:1635–1640.

674 Borghese J, Arduini D, Schimmenti E, Iaciofano D, Mikac B, Badalamenti F, Giangrande A, Gravina MF,
675 Musco L, BRUTTO SLO (2022) Assessment of the Sabellaria alveolata reefs' structural features along
676 the Southern coast of Sicily (Strait of Sicily, Mediterranean Sea). Mediterr Mar Sci 23:890–899.

677 Brandl SJ, Emslie MJ, Ceccarelli DM, T. Richards Z (2016) Habitat degradation increases functional
678 originality in highly diverse coral reef fish assemblages. Ecosphere 7:e01557.

679 Bremec C, Carcedo C, Piccolo MC, Dos Santos E, Fiori S (2013) Sabellaria nanella (Sabellariidae): from
680 solitary subtidal to intertidal reef-building worm at Monte Hermoso, Argentina (39 S, south-west
681 Atlantic). J Mar Biol Assoc United Kingdom 93:81–86.

682 Brock VE (1954) A preliminary report on a method of estimating reef fish populations. J Wildl Manage
683 18:297–308.

684 Brunier G, Oiry S, Gruet Y, Dubois SF, Barillé L (2022) Topographic Analysis of Intertidal Polychaete
685 Reefs (Sabellaria alveolata) at a Very High Spatial Resolution. Remote Sens 14:307.

686 Le Cam J-BB, Fournier J, Etienne S, Couden J (2011) The strength of biogenic sand reefs: Visco-elastic
687 behaviour of cement secreted by the tube building polychaete Sabellaria alveolata, Linnaeus, 1767.
688 Estuar Coast Shelf Sci 91:333–339.

689 Cantafaro A, Ardizzone G, Enea M, Ligas A, Colloca F (2017) Assessing the importance of nursery areas of
690 European hake (Merluccius merluccius) using a body condition index. Ecol Indic 81:383–389.

691 Casella E, Collin A, Harris D, Ferse S, Bejarano S, Parravicini V, Hench JL, Rovere A (2017) Mapping coral
692 reefs using consumer-grade drones and structure from motion photogrammetry techniques. Coral Reefs
693 36:269–275.

694 Chabot D, Dillon C, Ahmed O, Shemrock A (2017) Object-based analysis of UAS imagery to map emergent
695 and submerged invasive aquatic vegetation: a case study. J Unmanned Veh Syst 5:27–33.

696 Cheal AJ, Emslie MJ, Currey-Randall LM, Heupel MR (2021) Comparability and complementarity of reef
697 fish measures from underwater visual census (UVC) and baited remote underwater video stations
698 (BRUVS). J Environ Manage 289:112375.

699 Christensen MS (1978) TROPHIC RELATIONSHIPS IN JUVENILES OF THREE SPECIES OF. Fish Bull
700 76:389.

701 Cocheret De La Morinière E, Pollux BJA, Nagelkerken I, Van Der Velde G (2002) Post-settlement life cycle
702 migration patterns and habitat preference of coral reef fish that use seagrass and mangrove habitats as
703 nurseries. Estuar Coast Shelf Sci 55:309–321.

704 Collin A, Dubois S, James D, Houet T (2019) Improving Intertidal Reef Mapping Using UAV Surface, Red
705 Edge, and Near-Infrared Data. Drones 3:67.

706 Collin A, Dubois S, Ramambason C, Etienne S (2018a) Very high-resolution mapping of emerging biogenic
707 reefs using airborne optical imagery and neural network: the honeycomb worm (Sabellaria alveolata)
708 case study. Int J Remote Sens 39:5660–5675.

Collin A, Etienne S, Feunteun E (2017) VHR coastal bathymetry using WorldView-3: colour versus learner. Remote Sens Lett 8:1072–1081.

Collin A, Ramambason C, Pastol Y, Casella E, Rovere A, Thiault L, Espiau B, Siu G, Lerouvreur F, Nakamura N (2018b) Very high resolution mapping of coral reef state using airborne bathymetric LiDAR surface-intensity and drone imagery. Int J Remote Sens 39:5676–5688.

Copp GH, Kovác V (1996) When do fish with indirect development become juveniles? Can J Fish Aquat Sci 53:746–752.

Costa C, Cataudella S (2007) Relationship between shape and trophic ecology of selected species of Sparids of the Caprolace coastal lagoon (Central Tyrrhenian sea). Environ Biol Fishes 78:115–123.

Costanza R, Arge R, Groot R De, Farberk S, Grasso M, Hannon B, Limburg K, Naeem S, O'Neill R V, Paruelo J, Raskin RG, Suttonkk P, van den Belt M (1997) The value of the world ' s ecosystem services and natural capital. Nature 387:253–260.

Curd A, Chevalier M, Vasquez M, Boyé A, Firth LB, Marzloff MP, Bricheno LM, Burrows MT, Bush LE, Cordier C (2023) Applying landscape metrics to species distribution model predictions to characterize internal range structure and associated changes. Glob Chang Biol 29:631–647.

Curd A, Pernet F, Corporeau C, Delisle L, Firth LB, Nunes FLD, Dubois SF (2019) Connecting organic to mineral: How the physiological state of an ecosystem-engineer is linked to its habitat structure. Ecol Indic 98:49–60.

Curtis LA (1975) Distribution of Sabellaria vulgaris Verrill (Polychaeta: Sabellariidae) on a sandflat in Delaware Bay. Chesap Sci 16:14–19.

Dahlgren CP, Kellison GT, Adams AJ, Gillanders BM, Kendall MS, Layman CA, Ley JA, Nagelkerken I, Serafy JE (2006) Marine nurseries and effective juvenile habitats: concepts and applications. Mar Ecol Prog Ser 312:291–295.

Dance MA, Rooker JR (2016) Stage-specific variability in habitat associations of juvenile red drum across a latitudinal gradient. Mar Ecol Prog Ser 557:221–235.

Deias C, Guido A, Sanfilippo R, Apollaro C, Dominici R, Cipriani M, Barca D, Vespasiano G (2023) Elemental Fractionation in Sabellariidae (Polychaeta) Biocement and Comparison with Seawater Pattern: A New Environmental Proxy in a High-Biodiversity Ecosystem? Water 15:1549.

Desroy N, Dubois SF, Fournier J, Ricquiers L, Le Mao P, Guerin L, Gerla D, Rougerie M, Legendre A (2011) The conservation status of *Sabellaria alveolata (L.)* (Polychaeta: Sabellariidae) reefs in the Bay of Mont-Saint-Michel. Aquat Conserv Mar Freshw Ecosyst 21:462–471.

Dias AS, Paula JJJ (2001) Associated fauna of Sabellaria alveolata colonies on the central coast of Portugal. J Mar Biol Assoc United Kingdom 81:169–170.

Donnarumma L, D'Argenio A, Sandulli R, Russo GF, Chemello R (2021) Unmanned aerial vehicle technology to assess the state of threatened biogenic formations: The vermetid reefs of mediterranean intertidal rocky coasts. Estuar Coast Shelf Sci 251:107228.

Dorenbosch M, Van Riel MC, Nagelkerken I, Van der Velde G (2004) The relationship of reef fish densities to the proximity of mangrove and seagrass nurseries. Estuar Coast Shelf Sci 60:37–48.

Dubois S, Barillé L, Retière C (2003) Efficiency of particle retention and clearance rate in the polychaete Sabellaria alveolata L. C R Biol 326:413–421.

749 Dubois S, Commito JA, Olivier F, Retière C (2006) Effects of epibionts on Sabellaria alveolata (L.) biogenic
750 reefs and their associated fauna in the Bay of Mont Saint-Michel. Estuar Coast Shelf Sci 68:635–646.

751 Dubois S, Retière C, Olivier F (2002) Biodiversity associated with Sabellaria alveolata (Polychaeta:
752 Sabellariidae) reefs: Effects of human disturbances. J Mar Biol Assoc United Kingdom 82:817–826.

753 Edgar GJ, Barrett NS, Morton AJ (2004) Biases associated with the use of underwater visual census
754 techniques to quantify the density and size-structure of fish populations. J Exp Mar Bio Ecol 308:269–
755 290.

756 Egerton JP, Johnson AF, Turner J, LeVay L, Mascareñas-Osorio I, Aburto-Oropeza O (2018)
757 Hydroacoustics as a tool to examine the effects of Marine Protected Areas and habitat type on marine
758 fish communities. Sci Rep 8:47.

759 Esri R (2011) ArcGIS desktop: release 10. Environ Syst Res Institute, CA.

760 Ferraton F, Harmelin-Vivien M, Mellon-Duval C, Souplet A (2007) Spatio-temporal variation in diet may
761 affect condition and abundance of juvenile European hake in the Gulf of Lions (NW Mediterranean).
762 Mar Ecol Prog Ser 337:197–208.

763 Firth LB, Curd A, Hawkins SJ, Knights AM, Blaze JA, Burrows MT, Dubois SF, Edwards H, Foggo A,
764 Gribben PE (2021) On the diversity and distribution of a data deficient habitat in a poorly mapped
765 region: The case of Sabellaria alveolata L. in Ireland. Mar Environ Res 169:105344.

766 Firth LB, Mieszkowska N, Grant LM, Bush LE, Davies AJ, Frost MT, Moschella PS, Burrows MT,
767 Cunningham PN, Dye SR (2015) Historical comparisons reveal multiple drivers of decadal change of
768 an ecosystem engineer at the range edge. Ecol Evol 5:3210–3222.

769 Foody GM (2020) Explaining the unsuitability of the kappa coefficient in the assessment and comparison of
770 the accuracy of thematic maps obtained by image classification. Remote Sens Environ 239:111630.

771 Francour P (1997) Fish assemblages of Posidonia oceanica beds at Port-Cros (France, NW Mediterranean):
772 assessment of composition and long-term fluctuations by visual census. Mar Ecol 18:157–173.

773 Franzitta G, Colletti A, Savinelli B, Lo Martire M, Corinaldesi C, Musco L (2022) Feasibility of the
774 Sabellarid Reef Habitat Restoration. Front Mar Sci 9:349.

775 Friedlander AM, Parrish JD (1998) Habitat characteristics affecting fish assemblages on a Hawaiian coral
776 reef. J Exp Mar Bio Ecol 224:1–30.

777 Garcia-Rubies A, Macpherson E (1995) Substrate use and temporal pattern of recruiment in juvenile fishes
778 of the Mediterranean littoral. Mar Biol 124:35–42.

779 Giangrande A, Gambi MC, Gravina MF (2020) Polychaetes as habitat former: structure and function.
780 Perspect Mar Anim For World:219–237.

781 Gibb N, Tillin HM, Pearce B, Tyler-Walters H (2014) Assessing the sensitivity of Sabellaria spinulosa to
782 pressures associated with marine activities.

783 De Girolamo M, Mazzoldi C (2001) The application of visual census on Mediterranean rocky habitats. Mar
784 Environ Res 51:1–16.

785 Goncalves JA, Henriques R (2015) UAV photogrammetry for topographic monitoring of coastal areas.
786 ISPRS J Photogramm Remote Sens 104:101–111.

787 Gravina MF, Cardone F, Bonifazi A, Bertrandino MS, Chimienti G, Longo C, Marzano CN, Moretti M,

Lisco S, Moretti V, Corriero G, Giangrande A (2018) Sabellaria spinulosa (Polychaeta, Annelida) reefs in the Mediterranean Sea: Habitat mapping, dynamics and associated fauna for conservation management. Estuar Coast Shelf Sci 200:248–257.

Green SJ, Tamburello N, Miller SE, Akins JL, Côté IM (2013) Habitat complexity and fish size affect the detection of Indo-Pacific lionfish on invaded coral reefs. Coral reefs 32:413–421.

Guisan A, Zimmermann NE (2000) Predictive habitat distribution models in ecology. Ecol Modell 135:147–186.

Harmelin-Vivien ML, Harmelin JG, Chauvet C, Duval C, Galzin R, Lejeune P, Barnabé G, Blanc F, Chevalier R, Duclerc J (1985) Evaluation visuelle des peuplements et populations de poissons méthodes et problèmes. Rev d'écologie.

Harmelin-Vivien ML, Harmelin JG, Leboulleux V (1995) Microhabitat requirements for settlement of juvenile sparid fishes on Mediterranean rocky shores. Hydrobiologia 300–301:309–320.

Heck Jr KL, Hays G, Orth RJ, Heck KL, Hays G, Orth RJ (2003) Critical evaluation of the nursery role hypothesis for seagrass meadows. Mar Ecol Prog Ser 253:123–136.

Ingrosso G, Abbiati M, Badalamenti F, Bavestrello G, Belmonte G, Cannas R, Benedetti-Cecchi L, Bertolino M, Bevilacqua S, Bianchi CNCN, Bo M, Boscari E, Cardone F, Cattaneo-Vietti R, Cau A, Cerrano C, Chemello R, Chimienti G, Congiu L, Corriero G, Costantini F, De Leo F, Donnarumma L, Falace A, Fraschetti S, Giangrande A, Gravina MF, Guarnieri G, Mastrototaro F, Milazzo M, Morri C, Musco L, Pezzolesi L, Piraino S, Prada F, Ponti M, Rindi F, Russo GF, Sandulli R, Villamor A, Zane L, Boero F (2018) Mediterranean bioconstructions along the Italian coast. Adv Mar Biol 79:61–136.

Jackson-Bué T, Williams GJ, Walker-Springett G, Rowlands SJ, Davies AJ (2021) Three-dimensional mapping reveals scale-dependent dynamics in biogenic reef habitat structure. Remote Sens Ecol Conserv 7:621–637.

Jackson EL, Rowden AA, Attrill MJ, Bossey SJ, Jones MB (2001) The importance of seagrass beds as a habitat for fishery species. Oceanogr Mar Biol 39:269–304.

Jeong E, Park J-Y, Hwang C-S (2018) Assessment of UAV photogrammetric mapping accuracy in the beach environment. J Coast Res:176–180.

St. John J, Russ GR, Gladstone W (1990) Accuracy and bias of visual estimates of numbers, size structure and biomass of a coral reef fish. Mar Ecol Prog Ser:253–262.

Jones AG, Denis L, Fournier J, Desroy N, Duong G, Dubois SF (2020) Linking multiple facets of biodiversity and ecosystem functions in a coastal reef habitat. Mar Environ Res 162:105092.

Jones AG, Dubois SF, Desroy N, Fournier J (2018) Interplay between abiotic factors and species assemblages mediated by the ecosystem engineer Sabellaria alveolata (Annelida: Polychaeta). Estuar Coast Shelf Sci 200:1–18.

Jones AG, Dubois SF, Desroy N, Fournier J (2021) Intertidal ecosystem engineer species promote benthic-pelagic coupling and diversify trophic pathways. Mar Ecol Prog Ser 660:119–139.

Jones T, Davidson RJ, Gardner JPA, Bell JJ (2015) Evaluation and optimisation of underwater visual census monitoring for quantifying change in rocky-reef fish abundance. Biol Conserv 186:326–336.

Kassambara A (2020) Ggpubr:"ggplot2" based publication ready plots. R Packag version 04 0 438.

827 Kenny AJ, Cato I, Desprez M, Fader G, Schüttenhelm RTE, Side J (2003) An overview of seabed-mapping
828 technologies in the context of marine habitat classification. ICES J Mar Sci 60:411–418.

829 Kislik C, Genzoli L, Lyons A, Kelly M (2020) Application of UAV imagery to detect and quantify
830 submerged filamentous algae and rooted macrophytes in a non-wadeable river. Remote Sens 12:1–24.

831 Kulbicki M (1998) How the acquired behaviour of commercial reef fishes may influence the results obtained
832 from visual censuses. J Exp Mar Bio Ecol 222:11–30.

833 Lefcheck JS, Hughes BB, Johnson AJ, Pfirrmann BW, Rasher DB, Smyth AR, Williams BL, Beck MW,
834 Orth RJ (2019) Are coastal habitats important nurseries? A meta-analysis. Conserv Lett 12:e12645.

835 Lindsay JB (2014) The whitebox geospatial analysis tools project and open-access GIS. In: *Proceedings of*
836 *the GIS Research UK 22nd Annual Conference, The University of Glasgow*. p 16–18

837 Lisco S, Moretti M, Moretti V, Cardone F, Corriero G, Longo C (2017) Sedimentological features of
838 Sabellaria spinulosa biocontructions. Mar Pet Geol 87:203–212.

839 Litvin SY, Weinstein MP, Sheaves M, Nagelkerken I (2018) What makes nearshore habitats nurseries for
840 nekton? An emerging view of the nursery role hypothesis. Estuaries and Coasts 41:1539–1550.

841 Lloret J, Gil de Sola L, Souplet A, Galzin R (2002) Effects of large-scale habitat variability on condition of
842 demersal exploited fish in the north-western Mediterranean. ICES J Mar Sci 59:1215–1227.

843 Macpherson E (1998) Ontogenetic shifts in habitat use and aggregation in juvenile sparid fishes. J Exp Mar
844 Bio Ecol 220:127–150.

845 La Manna G, Guala I, Grech D, Perretti F, Ronchetti F, Manghi M, Ruiu A, Ceccherelli G (2021)
846 Performance of a baited underwater video system vs. the underwater visual census technique in
847 assessing the structure of fish assemblages in a Mediterranean marine protected area. Mediterr Mar Sci
848 22:480–495.

849 Méndez Casariego A, Schwindt E, Iribarne O (2004) Evidence of habitat structure-generated bottleneck in
850 the recruitment process of the SW Atlantic crab Cyrtograpsus angulatus. Mar Biol 145:259–264.

851 Moretti M, Lisco S, Brandano M, Tomassetti L, Gravina MF, Pantaloni M, Console F (2019) The Sabellaria
852 bioconstructions and their Plio-Pleistocene substratum along the southern Latium coast (Tor Caldara,
853 Anzio, Italy). In: *34th IAS Meeting of Sedimentology, Rome (Italy) September*. p 10–13

854 Muller A, Dubois SF, Boyé A, Becheler R, Droual G, Chevalier M, Pasquier M, Roudaut L, Fournier-
855 Sowinski J, Auby I (2023) Environmental filtering and biotic interactions act on different facets of the
856 diversity of benthic assemblages associated with eelgrass. Ecol Evol 13:e10159.

857 Muller A, Poitrimol C, Nunes FLD, Boyé A, Curd A, Desroy N, Firth LB, Bush L, Davies AJ, Lima FP
858 (2021) Musical chairs on temperate reefs: Species turnover and replacement within functional groups
859 explain regional diversity variation in assemblages associated with honeycomb worms. Front Mar Sci
860 8:654141.

861 Mumby PJ, Edwards AJ, Ernesto Arias-Gonzalez J, Lindeman KC, Blackwell PG, Gall A, Gorczynska MI,
862 Harborne AR, Pescod CL, Renken H (2004) Mangroves enhance the biomass of coral reef fish
863 communities in the Caribbean. Nature 427:533–536.

864 Murfitt SL, Allan BM, Bellgrove A, Rattray A, Young MA, Ierodiaconou D (2017) Applications of
865 unmanned aerial vehicles in intertidal reef monitoring. Sci Rep 7:10259.

Murphy HM, Jenkins GP (2010) Observational methods used in marine spatial monitoring of fishes and associated habitats: a review. Mar Freshw Res 61:236–252.

Nagelkerken I (2009) Evaluation of nursery function of mangroves and seagrass beds for tropical decapods and reef fishes: patterns and underlying mechanisms. Ecol Connect among Trop Coast Ecosyst:357–399.

Nagelkerken I, Roberts CM vd, Van Der Velde G, Dorenbosch M, Van Riel MC, De La Moriniere EC, Nienhuis PH (2002) How important are mangroves and seagrass beds for coral-reef fish? The nursery hypothesis tested on an island scale. Mar Ecol Prog Ser 244:299–305.

Nagelkerken I, Sheaves M, Baker R, Connolly RM (2015) The seascape nursery: a novel spatial approach to identify and manage nurseries for coastal marine fauna. Fish Fish 16:362–371.

Nguyen T, Liquet B, Mengersen K, Sous D (2021) Mapping of coral reefs with multispectral satellites: a review of recent papers. Remote Sens 13:4470.

Olán-González M, Briones-Fourzán P, Lozano-Álvarez E, Acosta-González G, Alvarez-Filip L (2023) Similar functional composition of fish assemblages despite contrasting levels of habitat degradation on shallow Caribbean coral reefs. PLoS One 18:e0295238.

Pais MP, Cabral HN (2018) Effect of underwater visual survey methodology on bias and precision of fish counts: a simulation approach. PeerJ 6:e5378.

Pais MP, Cabral HN (2017) Fish behaviour effects on the accuracy and precision of underwater visual census surveys. A virtual ecologist approach using an individual-based model. Ecol Modell 346:58–69.

Papakonstantinou A, Topouzelis K, Pavlogeorgatos G (2016) Coastline Zones Identification and 3D Coastal Mapping Using UAV Spatial Data. ISPRS Int J Geo-Information 5:75.

Le Pape O, Bonhommeau S (2015) The food limitation hypothesis for juvenile marine fish. Fish Fish 16:373–398.

Paterson AW, Whitfield AK (2000) Do shallow-water habitats function as refugia for juvenile fishes? Estuar Coast Shelf Sci 51:359–364.

Pearce B, Hill JM, Grubb L, Harper G (2011a) Impacts of marine aggregate dredging on adjacent Sabellaria spinulosa aggregations and other benthic fauna. Mar Aggregates Levy Sustain Fund MEPF 8:P39.

Pearce B, Hill JM, Wilson C, Griffin R, Earnshaw S, Pitts J (2011b) Sabellaria spinulosa Reef Ecology and Ecosystem Services. Crown Estate (120 pp).

La Porta BN, Luisa, Nicoletti L (2009) Sabellaria alveolata (Linnaeus) reefs in the central Tyrrhenian Sea (Italy) and associated polychaete fauna. Zoosymposia 2:527–536.

Rabaut M, Van de Moortel L, Vincx M, Degraer S (2010) Biogenic reefs as structuring factor in Pleuronectes platessa (Plaice) nursery. J Sea Res 64:102–106.

Rabaut M, Vincx M, Degraer S (2009) Do Lanice conchilega (sandmason) aggregations classify as reefs? Quantifying habitat modifying effects. Helgol Mar Res 63:37–46.

Reise K (2012) Tidal flat ecology: an experimental approach to species interactions. Springer Science & Business Media.

Ribeiro C, Almeida AJ, Araújo R, Biscoito M, Freitas M (2005) Fish assemblages of Cais do Carvao Bay (Madeira Island) determined by the visual census technique. J Fish Biol 67:1568–1584.

905 Rossiter T, Furey T, McCarthy T, Stengel DB (2020) UAV-mounted hyperspectral mapping of intertidal
906 macroalgae. Estuar Coast Shelf Sci 242:106789.

907 Ruiz GM, Hines AH, Posey MH (1993) Shallow water as a refuge habitat for fish and crustaceans in non-
908 vegetated estuaries: an example from Chesapeake Bay. Mar Ecol Prog Ser:1–16.

909 Russo T, Costa C, Cataudella S (2007) Correspondence between shape and feeding habit changes throughout
910 ontogeny of gilthead sea bream Sparus aurata L., 1758. J Fish Biol 71:629–656.

911 Sala E, Ballesteros E (1997) Partitioning of space and food resources by three fish of the genus Diplodus
912 (Sparidae) in a Mediterranean rocky infralittoral ecosystem. Mar Ecol Prog Ser 152:273–283.

913 Sale PF, Douglas WA (1981) Precision and accuracy of visual census technique for fish assemblages on
914 coral patch reefs. Environ Biol Fishes 6:333–339.

915 Sanfilippo R, Serio D, Deias C, Rosso A (2022) Sabellaria alveolata (Annelida, Polychaeta) bioconstructions
916 and associated macroalgal community from Portopalo di Capo Passero (SE Sicily). Mediterr Mar Sci
917 23:150–156.

918 Schloesser RW, Fabrizio MC (2019) Nursery habitat quality assessed by the condition of juvenile fishes: not
919 all estuarine areas are equal. Estuaries and Coasts 42:548–566.

920 Searcy SP, Eggleston DB, Hare JA (2007) Is growth a reliable indicator of habitat quality and essential fish
921 habitat for a juvenile estuarine fish? Can J Fish Aquat Sci 64:681–691.

922 Seitz RD, Wennhage H, Bergström U, Lipcius RN, Ysebaert T (2014) Ecological value of coastal habitats
923 for commercially and ecologically important species. ICES J Mar Sci 71:648–665.

924 Sheaves M, Baker R, Johnston R (2006) Marine nurseries and effective juvenile habitats: an alternative view.
925 Mar Ecol Prog Ser 318:303–306.

926 Stone R, Callaway R, Bull JC (2019) Are biodiversity offsetting targets of ecological equivalence feasible
927 for biogenic reef habitats? Ocean Coast Manag 177:97–111.

928 Tait LW, Orchard S, Schiel DR (2021) Missing the forest and the trees: Utility, limits and caveats for drone
929 imaging of coastal marine ecosystems. Remote Sens 13:3136.

930 Tillin HM, Gibb N (2018) Sabellaria spinulosa, didemnids and other small ascidians on tide-swept
931 moderately wave-exposed circalittoral rock.

932 Tiralongo F, Mancini E, Ventura D, Malherbe SDESDE, Mendoza FPDEFPDE, Sardone M, Arciprete R,
933 Massi D, Marcelli M, Fiorentino F, Fiorentino F, Minervini R (2021) Commercial Catches And
934 Discards Composition In The Central Tyrrhenian Sea: A Multispecies Quantitative And Qualitative
935 Analysis From Shallow And Deep Bottom Trawling. Mediterr Mar Sci 22:521–531.

936 Ventura D, Bonhomme V, Colangelo P, Bonifazi A, Jona Lasinio G, Ardizzone G (2017) Does morphology
937 predict trophic niche differentiation? Relationship between feeding habits and body shape in four co-
938 occurring juvenile species (Pisces: Perciformes, Sparidae). Estuar Coast Shelf Sci 191:84–95.

939 Ventura D, Bonifazi A, Gravina MF, Belluscio A, Ardizzone G (2018a) Mapping and classification of
940 ecologically sensitive marine habitats using unmanned aerial vehicle (UAV) imagery and Object-Based
941 Image Analysis (OBIA). Remote Sens 10.

942 Ventura D, Bonifazi A, Lasinio GJGJGJGJGJ, Gravina MFMFMFMFMF, Mancini E, Ardizzone G (2018b)
943 Can microscale habitat-related differences influence the abundance of ectoparasites ? Multiple

evidences from two juvenile coastal fish (Perciformes: Sparidae). Estuar Coast Shelf Sci 209:110–122.

Ventura D, Bruno M, Jona Lasinio G, Belluscio A, Ardizzone G (2016) A low-cost drone based application for identifying and mapping of coastal fish nursery grounds. Estuar Coast Shelf Sci 171:85–98.

Ventura D, Dubois SF, Bonifazi A, Jona Lasinio G, Seminara M, Gravina MF, Ardizzone G (2021) Integration of close-range underwater photogrammetry with inspection and mesh processing software: a novel approach for quantifying ecological dynamics of temperate biogenic reefs. Remote Sens Ecol Conserv 7:169–186.

Ventura D, Grosso L, Pensa D, Casoli E, Mancini G, Valente T, Scardi M, Rakaj A (2023a) Coastal benthic habitat mapping and monitoring by integrating aerial and water surface low-cost drones. Front Mar Sci 9.

Ventura D, Grosso L, Pensa D, Casoli E, Mancini G, Valente T, Scardi M, Rakaj A (2023b) Coastal benthic habitat mapping and monitoring by integrating aerial and water surface low-cost drones. Front Mar Sci 9:1–15.

Ventura D, Jona Lasinio G, Ardizzone G (2015) Temporal partitioning of microhabitat use among four juvenile fish species of the genus Diplodus (Pisces: Perciformes, Sparidae). Mar Ecol 36:1013–1032.

Ventura D, Napoleone F, Cannucci S, Alleaume S, Valentini E, Casoli E, Burrascano S (2022) Integrating low-altitude drone based-imagery and OBIA for mapping and manage semi natural grassland habitats. J Environ Manage 321.

Vigliola L, Harmelin-Vivien M (2001) Post-settlement ontogeny in three Mediterranean reef fish species of the genus Diplodus. Bull Mar Sci 68:271–286.

Vigliola L, Harmelin-Vivien ML, Biagi F, Galzin R, Garcia-Rubies A, Harmelin JG, Jouvenel JY, Direach-Boursier L Le, Macpherson E, Tunesi L (1998) Spatial and temporal patterns of settlement among sparid fishes of the genus Diplodus in the northwestern Mediterranean. Mar Ecol Prog Ser 168:45–56.

Wetz JJ, Ajemian MJ, Shipley B, Stunz GW (2020) An assessment of two visual survey methods for documenting fish community structure on artificial platform reefs in the Gulf of Mexico. Fish Res 225:105492.

Wood S, Wood MS (2015) Package ‘mgcv’. R Packag version 1:729.

Wood SN (2001) Mgcv: GAMs and generalized ridge regression for R. R news 1:20–25.

Zuur AF, Ieno EN, Smith GM (2007) Analysing ecological data. Springer.

974 **TABLES**

975 **Table 1:** Site overall extent (m^2) and reef habitat cover (%) in the three sites (S1, S2, S3) as derived
976 from UAV-based aerial imagery OBIA classification.

977

Site (m^2)	Season	Habitat m^2 (% cover)		
		***Sabellaria* reef**	**Sandy bottoms**	**Rocks with algae**
S1 (6100)	Summer	2056.4 (33.4)	4067.2 (66.1)	27.9 (0.5)
	Winter	1406.2 (23)	4709 (77)	0 (0)
S2 (2700)	Summer	354 (12.9)	2229.4 (81.4)	155.5 (5.7)
	Winter	267.6 (9.8)	2448.5 (89.5)	18.6 (0.7)
S3 (4100)	Summer	227.3 (7.2)	813.5 (25.9)	3103.1 (66.9)
	Winter	203.8 (3.3)	982.4 (29.7)	2954.5 (67)

978

979 **Table 2:** Output of the GAM model on log-transformed juvenile densities (expressed in number of
980 juveniles per 100 m^2), reporting the model's linear and non-linear terms. Significant p-values are
981 highlighted in bold.

Linear terms				
Explanatory variable	**Estimate**	**Std. Error**	**t value**	**P-value**
Intercept	4.4059	0.2326	18.944	**<0.001**
Site: S2	-0.507	0.2446	-2.073	**0.039**
Site: S3	-0.7244	0.2388	-3.033	**0.003**
Species: *D. labrax*	-2.6066	0.2904	-8.975	**<0.001**
Species: *D. puntazzo*	-2.211	0.225	-9.828	**<0.001**
Species: *D. sargus*	-2.4086	0.1857	-12.97	**<0.001**
Species: *D. vulgaris*	-1.0024	0.2196	-4.565	**<0.001**
Species: S. salpa	-0.5664	0.2616	-2.165	**0.031**
Species: *U. cirrosa*	-1.8902	0.3736	-5.059	**<0.001**
Size class: Medium	-0.3964	0.1143	-3.469	**<0.001**
Size class: Large	-0.6955	0.1516	-4.587	**<0.001**
Non-linear (smooth) terms				
Explanatory variable	**edf**	**Ref. df**	**F**	**p-value**
CR (*Sabellaria* reef complexity Ratio)	3.38	3.78	2.605	**0.0218**

983

FIGURES

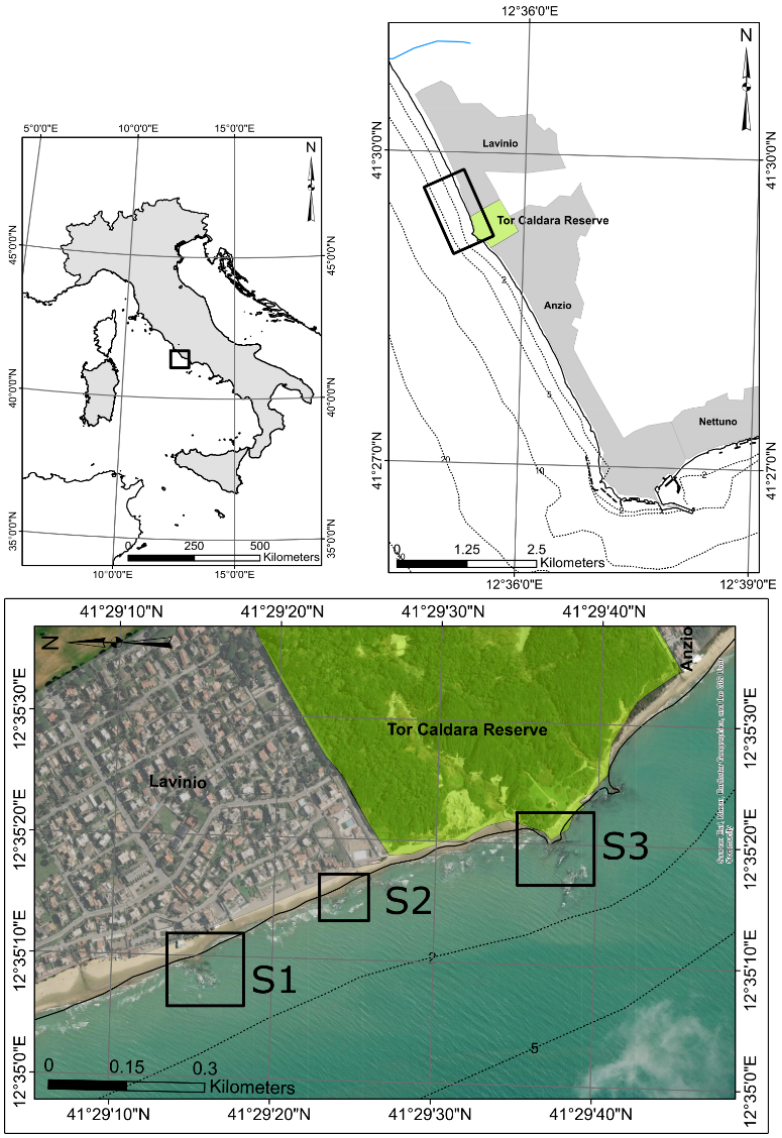

Figure 1: Map of the Latium coast south of Rome (Central Tyrrhenian Sea) where the three study sites (S1, S2, S3) were located. The main urban complex and the limit of the Tor Caldara Natural Reserve are reported by grey and green polygons, respectively. The dotted lines represent bathymetric depth contours.

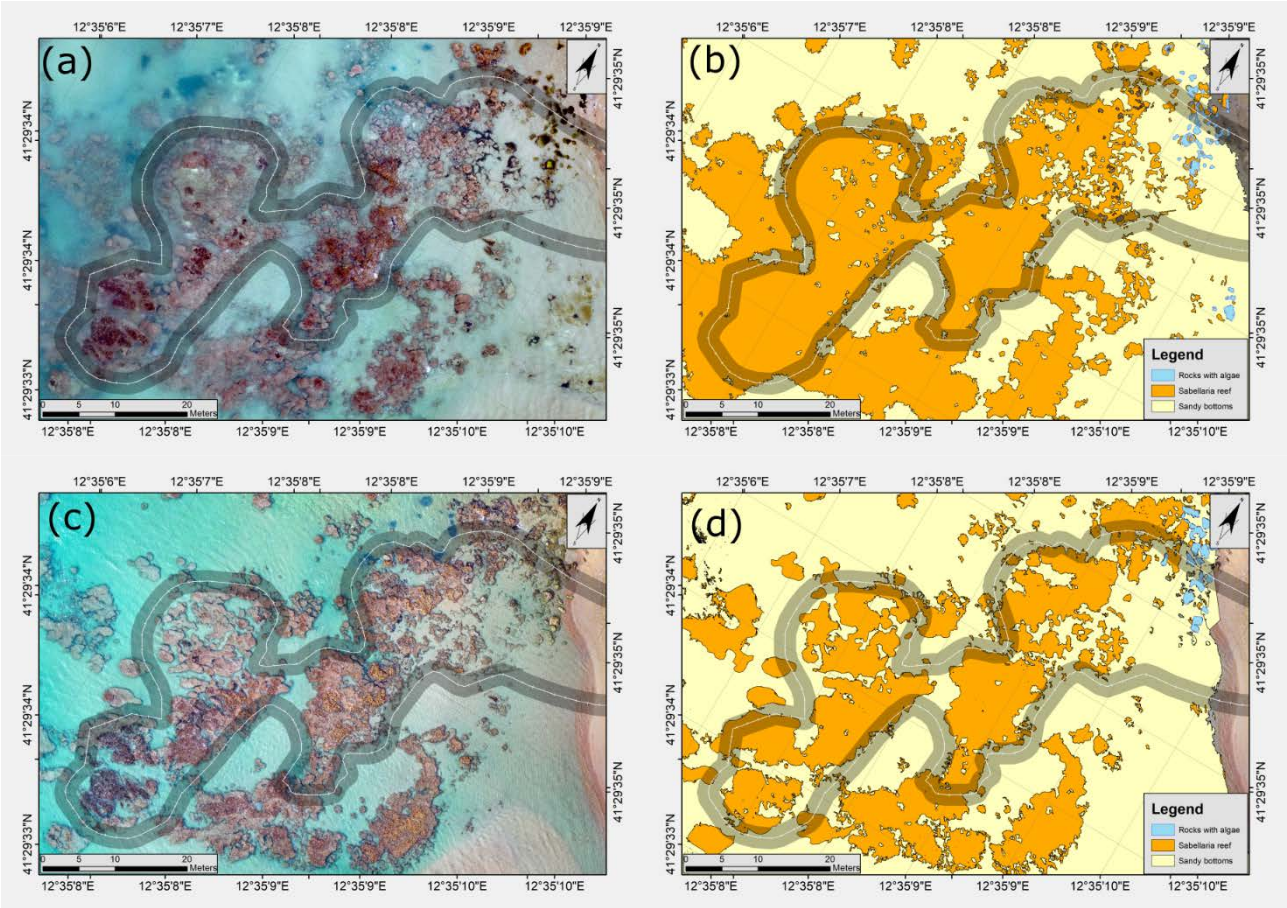

994

995 **Figure 2**: High spatial resolution mapping of *Sabellaria* reef using Unmanned Aerial Vehicles (UAV)-
996 based orthophotmosaic and imagery classification. Orthophoto mosaic of the S1 site in summer (a)
997 with the resulting classification derived by object-based image analysis (OBIA) leading to feature
998 extraction and identification of the three main seabed cover classes (rocks with algae, *S. alveolata*
999 reef and sandy bottoms) (b). Orthophoto mosaic of the S1 site in winter (c) with the resulting
1000 classification based on OBIA(d). Note the modification of reef boundaries and cover. The mean
1001 snorkeler's underwater visual census (UVC) path with a covered area of 600 m^2 (200 m Length x 3
1002 m Width) derived by multiple global positioning systems (GPS) tracks interpolation is reported in
1003 grey. The mapping and OBIA results of the S2 and S3 sites were reported in Fig. S1 as supplementary
1004 material.

1005

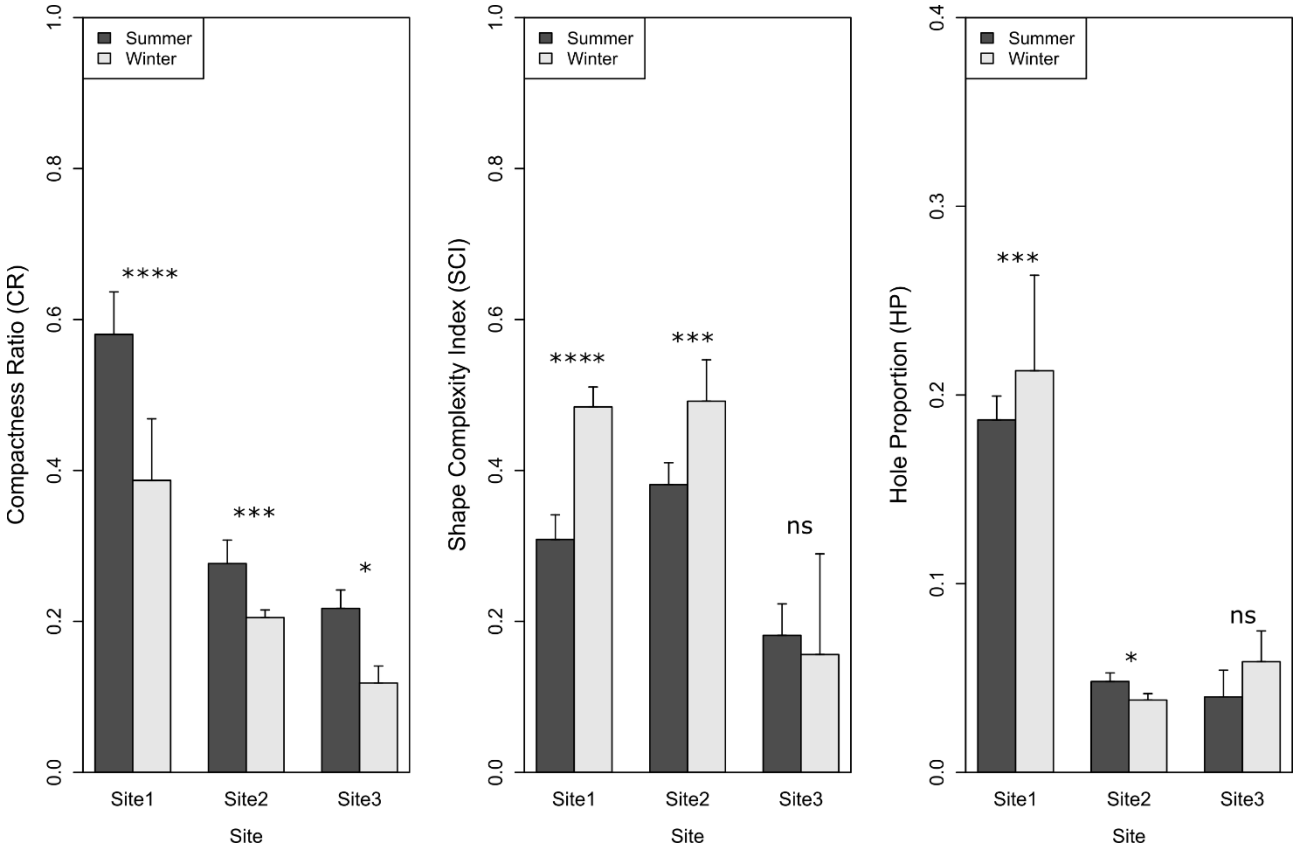

Figure 3: Mean values (± SE) of *Sabellaria alveolata* polygons-related reef metrics estimated after OBIA classification of UAV-based imagery. CR = Compactness ratio, SCI = Shape complexity, HP = Hole proportion. The Wilcoxon signed rank tests were used for pairwise comparisons. The alpha value was set at 0.05, and the Bonferroni adjustment was applied for multiple comparison. Significance codes: ****p <0.0001; ***p < 0.001; *p < 0.05; ns = non-significant. See Fig. 1 and Fig. S1 in the supplementary materials for mapping results and visualization of *S. alveolata* reef polygons over seasons.

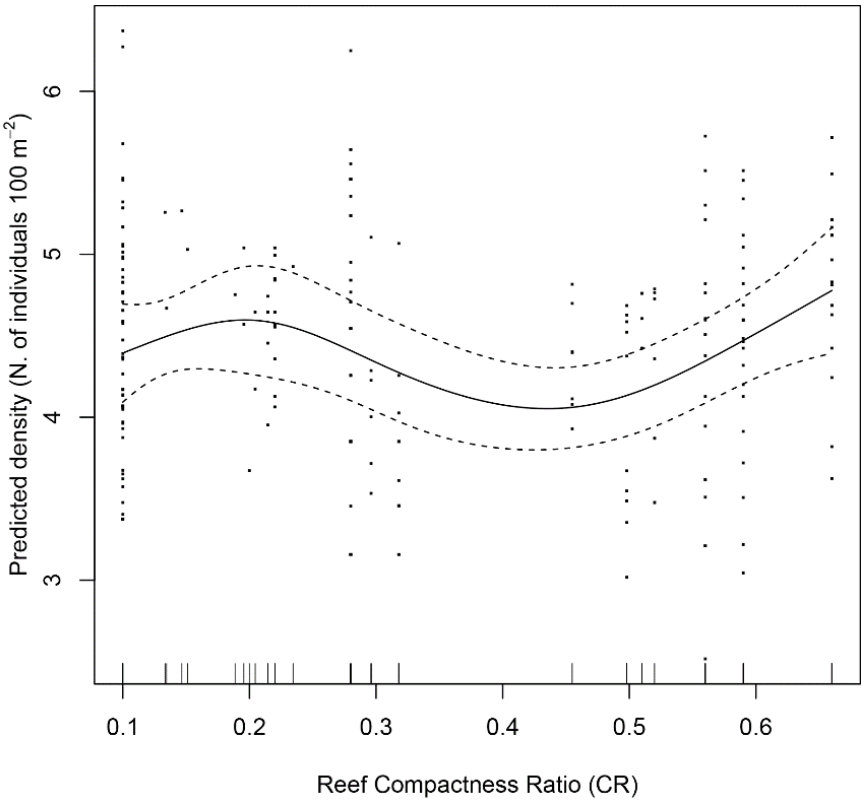

1015

1016 **Figure 4**: Response plots showing the influence of the retained non-linear term (*S. alveolata* reef
1017 Compactness Ratio, CR) on juvenile fish densities among the three sites according to the final
1018 generalized additive model (GAM). Model fit was assessed with Akaike's information criterion (AIC)
1019 and % deviance explained (DE). Solid lines represent smoothed values, and dotted lines represent
1020 95% confidence intervals. N = 256 observations (site x species x size classes).

1021

1022

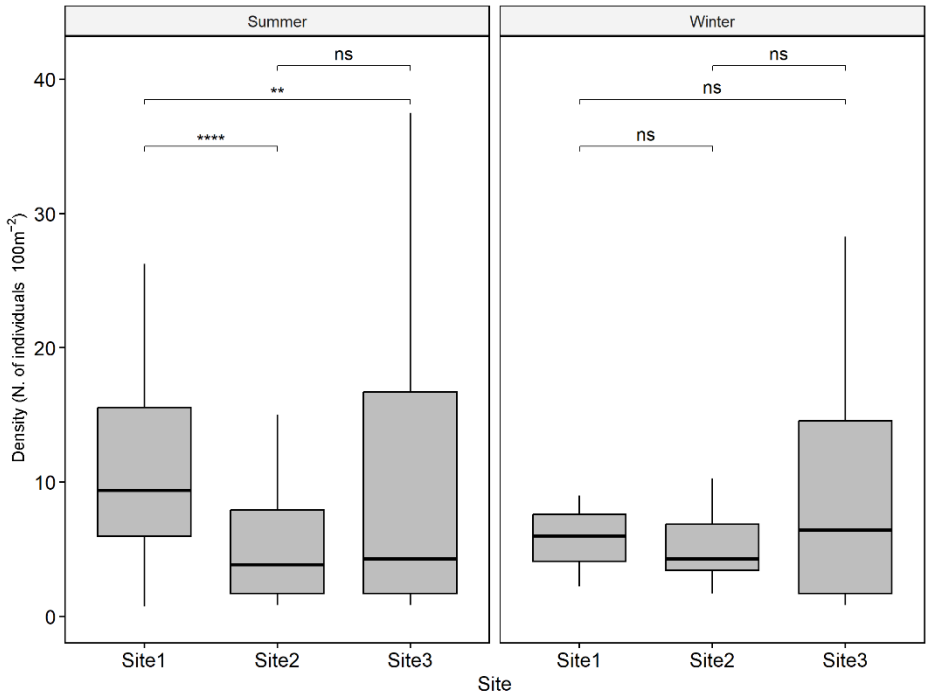

Figure 5: Seasonal variation in juvenile fish densities (expressed as N. of individuals per 100 m^2) recorded in the three sites from October 2020 to November 2021. The Wilcoxon signed rank tests were used for pairwise comparisons. The alpha value was set at 0.05, and the Bonferroni adjustment was applied for multiple comparison Significance codes: ****p <0.0001 = 0; **p < 0.01; ns = non-significant.

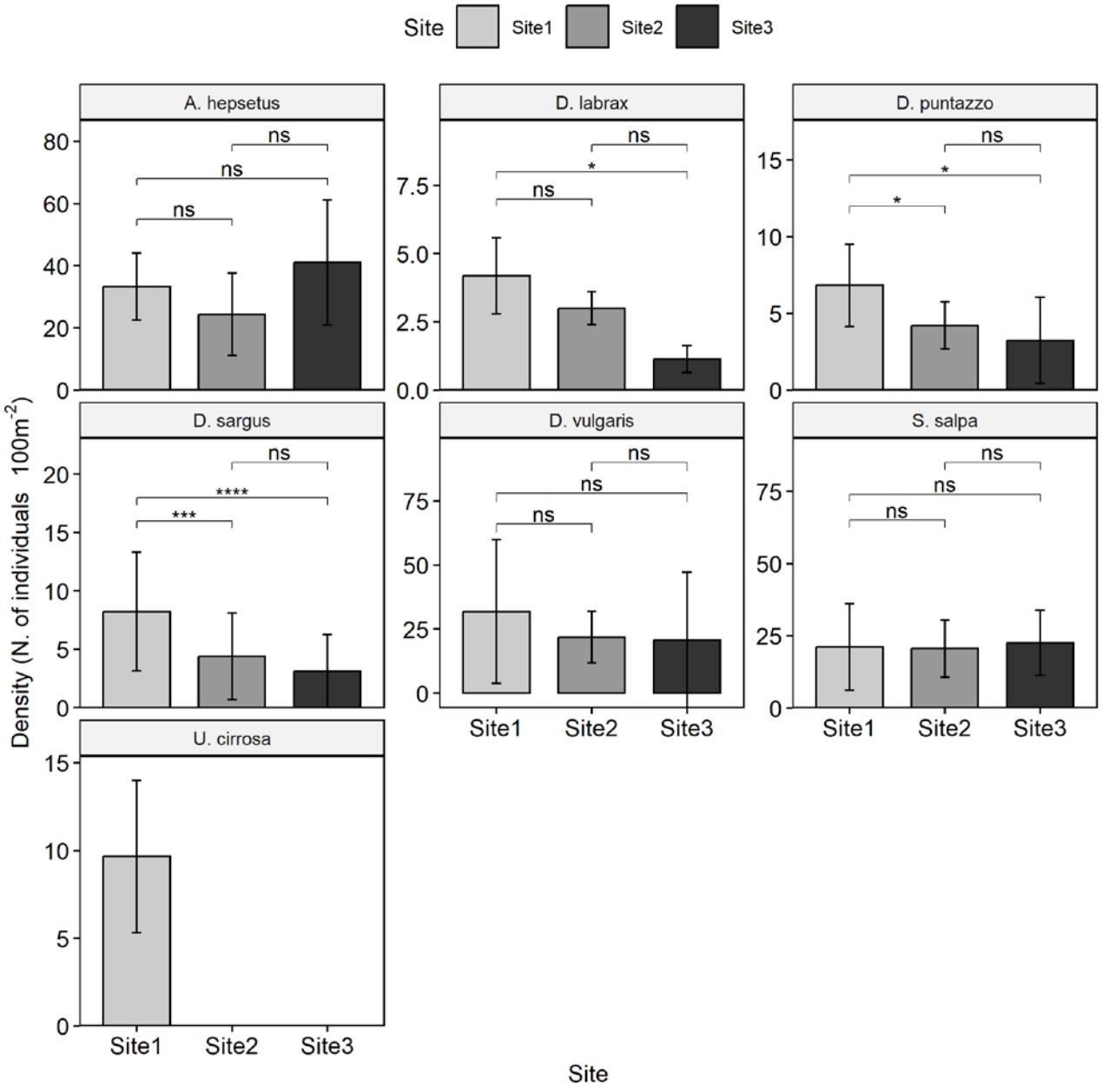

Figure 6: Mean (± SE) juvenile densities (expressed as N. of individuals per 100 m^2) of the seven fish species recorded in the three sites from October 2020 to November 2021. The Wilcoxon signed rank tests were used for pairwise comparisons. The alpha value was set at 0.05, and the Bonferroni adjustment was applied for multiple comparisons. Significance codes: ****P <0.0001; *P < 0.05; ns = non-significant.

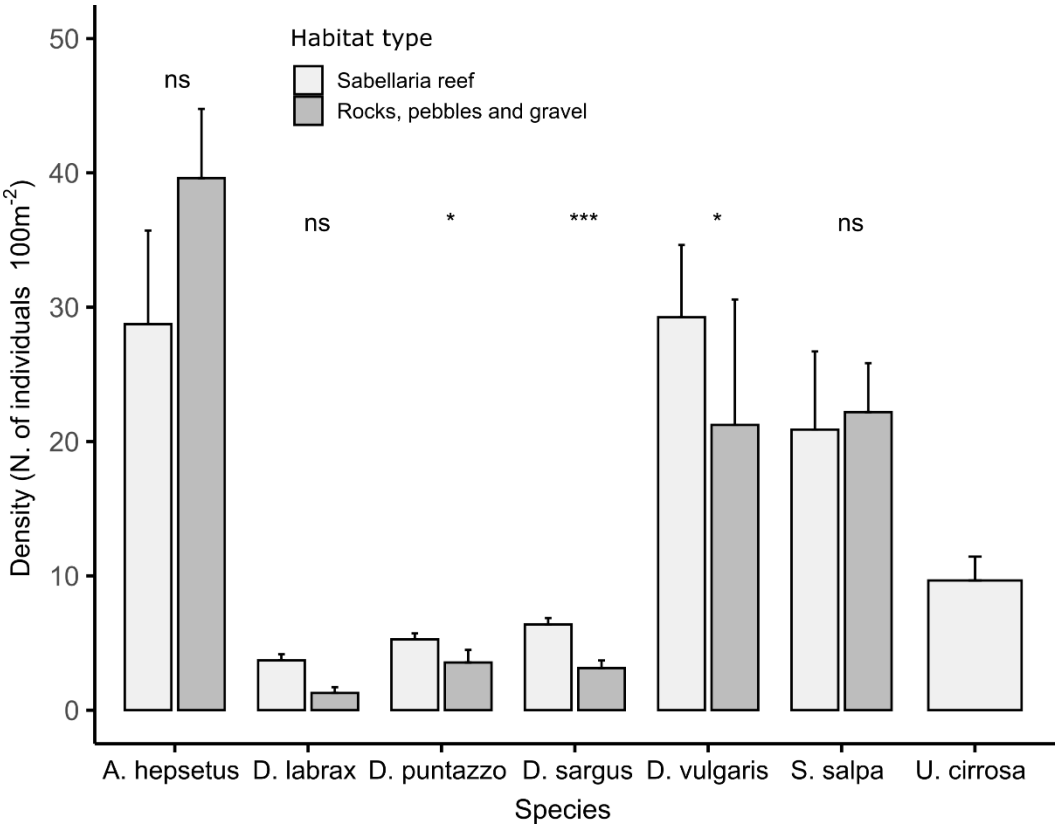

1037

1038 **Figure 7**: Mean (±SE) juvenile densities (expressed as N. of individuals per 100 m^2) of the seven

1039 species recorded in relation to preferential habitat use. The Wilcoxon signed rank tests were used

1040 for pairwise comparisons. The alpha value was set at 0.05, and the Bonferroni adjustment was

1041 applied for multiple comparisons. Significance codes: ****p <0.0001; *p < 0.05; ns = non-significant.

1042

1043

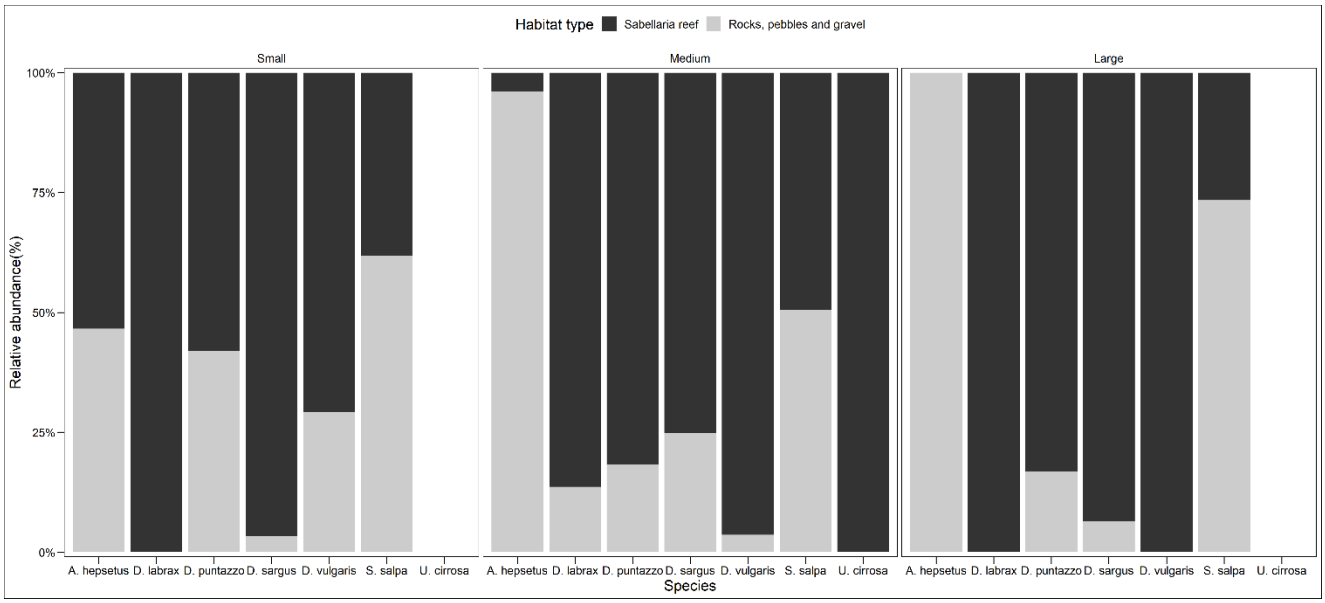

Figure 8: Relative abundance (expressed as %) of the seven juveniles species recorded in the three study sites (S1-S3), according to habitat type (i.e. *Sabellria alveolata* formations and other rocky substrates) and their size class (small, medium, and large).

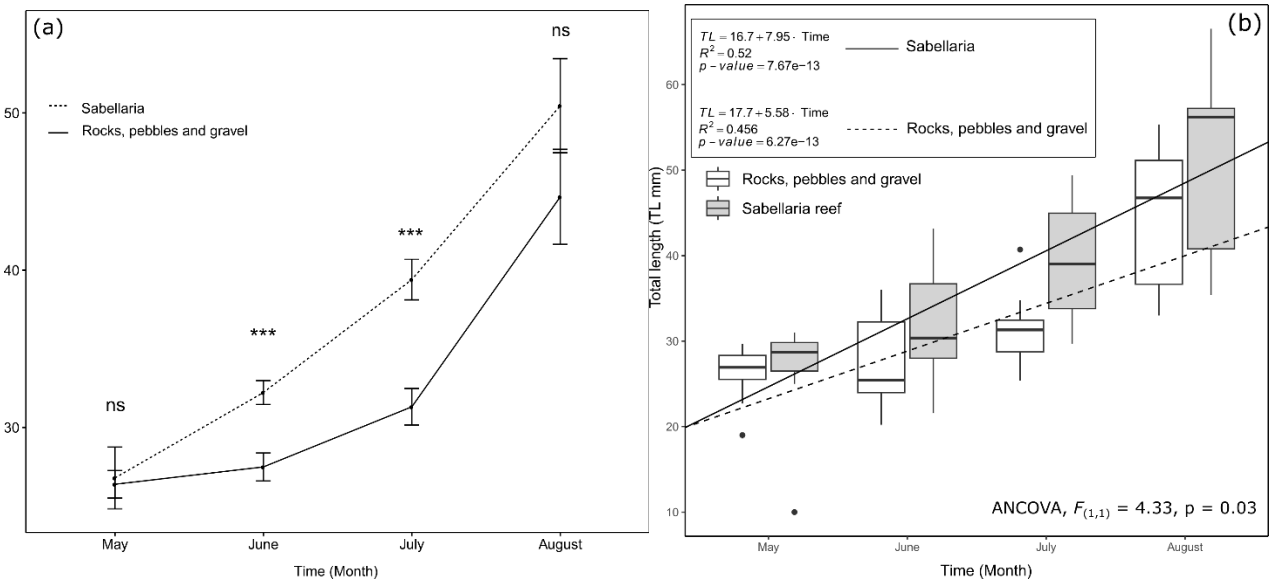

Figure 9: Monthly mean size (total length TL mm ± SE) variation of *Diplodus sargus* juveniles (N = 173) according to preferential substrate type from the arrival of juveniles (May) until dispersal outside the surveyed sites (August). (a) Line plot showing the mean size variation over time (month), the Wilcoxon signed rank tests were used for pairwise comparisons. The alpha value was set at 0.05,

and the Bonferroni adjustment was applied for multiple comparisons (Significance codes: ***p < 0.001; ns = non-significant). (b) Boxplot of the TL with superimposed regression lines between the two substrate types reporting significant differences in slopes (rate of change in TL) tested with ANCOVA. Values per habitat type were obtained by combining all size measurements of sampled specimens from Site S1 and S2 for *Sabellaria alveolata* reef and Site S3 for hard substrates (i.e. rocks, pebbles, and gravel), respectively, over the entire 2-year study period.

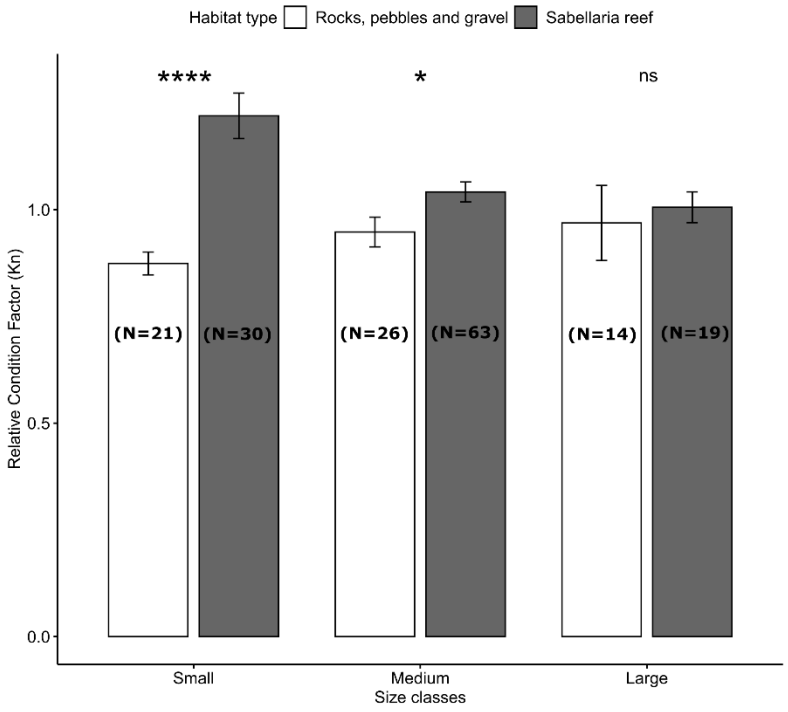

Figure 10: Mean (± SE) relative condition factor (K_n) of *Diplodus sargus* juveniles grouped by size class and habitat type. The Wilcoxon signed rank tests were used for pairwise comparisons. The alpha value was set at 0.05, and the Bonferroni adjustment was applied for multiple comparisons. Significance codes: ****p <0.0001; *P < 0.05; ns = non-significant. Values in parentheses indicate sample size.